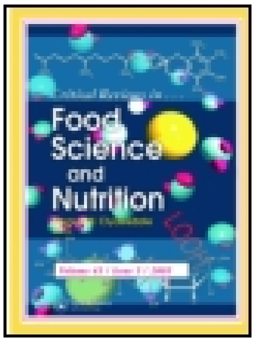

Critical Reviews in Food Science and Nutrition

ISSN: (Print) (Online) Journal homepage: https://www.tandfonline.com/loi/bfsn20

Phytosterols and phytostanols and the hallmarks of cancer in model organisms: A systematic review and meta-analysis

Giorgia Cioccoloni , Chrysa Soteriou , Alex Websdale , Lewis Wallis , Michael A. Zulyniak & James L. Thorne

CRITICAL REVIEWS IN FOOD SCIENCE AND NUTRITION
https://doi.org/10.1080/10408398.2020.1835820

REVIEW

OPEN ACCESS Check for updates

Phytosterols and phytostanols and the hallmarks of cancer in model organisms: A systematic review and meta-analysis

Giorgia Cioccoloni, Chrysa Soteriou, Alex Websdale, Lewis Wallis, Michael A. Zulyniak, and James L. Thorne

Food Science & Nutrition, University of Leeds, Leeds, West Yorkshire, UK

ABSTRACT

Phytosterols and phytostanols are natural products present in vegetable oils, nuts, and seeds, or added to consumer food products whose intake is inversely associated with incidence and prognosis of several cancers. Randomized cancer prevention trials in humans are unfeasible due to time and cost yet the cellular processes and signaling cascades that underpin anti-cancer effects of these phytochemicals have been explored extensively in vitro and in preclinical in vivo models. Here we have performed an original systematic review, meta-analysis, and qualitative interpretation of literature published up to June 2020. MEDLINE, Scopus, and hand-searching identified 408 unique records that were screened leading to 32 original articles that had investigated the effects of phytosterols or phytostanols on cancer biology in preclinical models. Data was extracted from 22 publications for meta-analysis. Phytosterols were most commonly studied and found to reduce primary and metastatic tumor burden in all cancer sites evaluated. Expression of pAKT, and markers of metastasis (alkaline phosphatase, matrix metalloproteases, epithelial to mesenchymal transcription factors, lung and brain colonization), angiogenesis (vascular endothelial growth factor, CD31), and proliferation (Ki67, proliferating cell nuclear antigen) were consistently reduced by phytosterol treatment in breast and colorectal cancer. Very high dose treatment (equivalent to 0.2–1 g/kg body weight not easily achievable through diet or supplementation in humans) was associated with adverse events including poor gut health and intestinal adenoma development. Phytosterols and phytostanols are already clinically recommended for cardiovascular disease risk reduction, and represent promising anti-cancer agents that could be delivered in clinic and to the general population at low cost, with a well understood safety profile, and now with a robust understanding of mechanism-of-action.

GRAPHICAL ABSTRACT

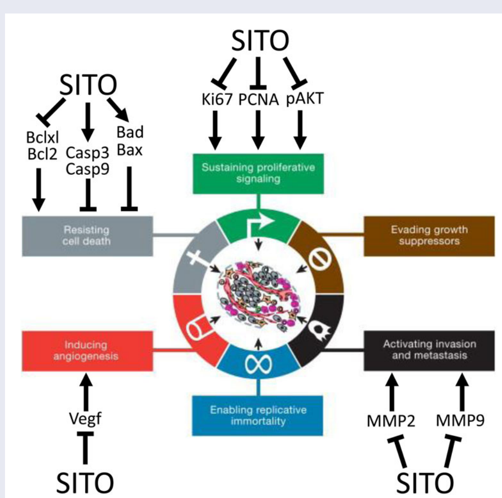

KEYWORDS
Phytosterol; phytostanol; cancer; neoplasm; cancer hallmarks; molecular mechanism

CONTACT J. L. Thorne j.l.thorne@leeds.ac.uk Food Science & Nutrition, University of Leeds, Leeds, West Yorkshire LS2 9JT, UK.

The graphical abstract is reprinted from *Cell*, vol. 144, issue 5, by Douglas Hanahan and Robert A. Weinberg, "Hallmarks of Cancer: The Next Generation", pages 646–674, © 2011, with permission from Elsevier.

Supplemental data for this article can be accessed at https://doi.org/10.1080/10408398.2020.1835820.

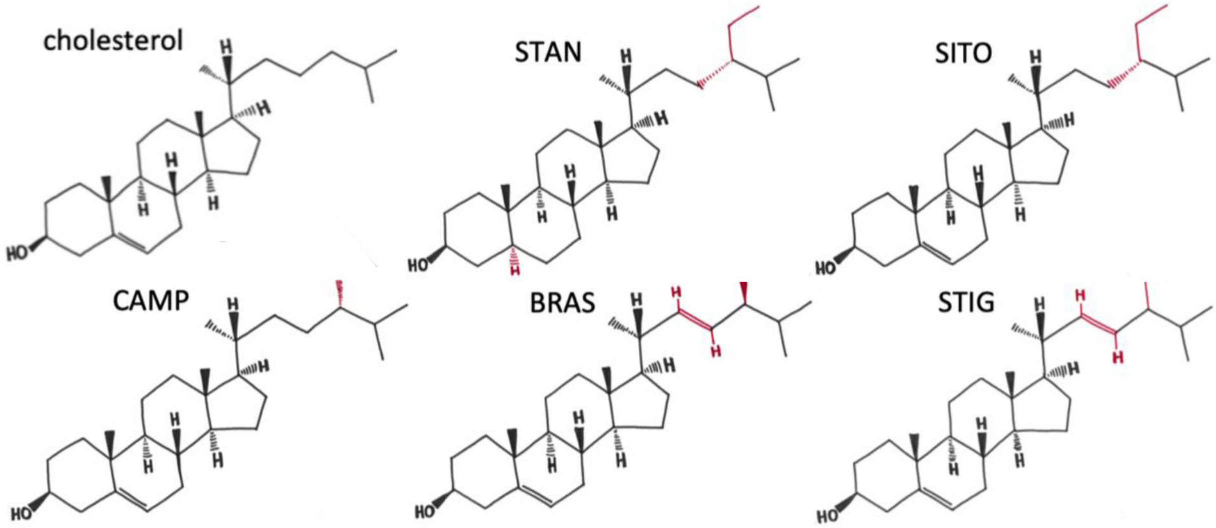

Figure 1. Molecular structure of cholesterol and common dietary plant sterols and stanols. Reproduced from (Hutchinson et al. 2019) with permission.

Introduction

Dietary intake of fruits and vegetables, and of grains and seeds, is inversely associated with cancer risk and directly associated with cancer patient survival (WCRF/AICR 2018). Research that provides mechanistic explanations for these epidemiological and clinical trial observations is incomplete, which limits translation for public health. One group of phytochemicals with proposed anti-cancer activity are phytosterols and their saturated counterparts, phytostanols. Case-control studies indicated that high dietary phytosterol/stanol (PSS) intake has been associated with reduced odds of several cancers including lung (odds ratio (OR) 0.29, 95% CI 0.14–0.63) (Mendilaharsu et al. 1998), stomach (OR 0.33, 95% CI 0.17–0.65) (De Stefani et al. 2000), colorectum (OR 0.50, 95% CI 0.41–0.61) (Huang et al. 2017), and ovary (OR 0.42, 95% CI 0.20–0.87) (McCann et al. 2003). A recent meta-analysis indicated PSS intake imparts a non-linear reduction in pan-cancer relative risk (RR 0.63, 95% CI 0.49–0.81) with peak reduction achieved with approximately 0.5 g/day or 6–7 mg/kg (Jiang et al. 2019).

Phytosterols, structurally and functionally related to cholesterol (Figure 1), are present in relatively large amounts in vegetable oils, nuts and seeds (Phillips et al. 2005) with the total phytosterol content of some vegetable oils reaching values as high as 19 g/kg (Yang et al. 2019). The richest sources are commercial products supplemented with PSS (approx. 2–3 g PSS per portion) that are marketed for lowering low density lipoprotein cholesterol (LDL-C), and do so by 10–15% in addition to what is achievable by statins (EFSA Panel on Dietetic Products, Nutrition and Allergies 2013; Han et al. 2016). Large scale manufacturing of PSS has standardized production methods which has ameliorated many problems commonly associated with studying natural products, where isolation, extraction, or synthesis methodology may vary, and final compounds applied in studies may be variable.

In 2000, Hanahan and Weinberg published 'The Hallmarks of Cancer' highlighting key characteristics of the developing tumor (Hanahan and Weinberg 2000). Here, we use the updated categorization (Hanahan and Weinberg 2011) to map how PSS may be interacting with cancerous and pre-cancerous cells in pre-clinical cancer models. This systematic review addresses a critical gap in the literature by collating all available information regarding the cellular and molecular response of tumors to PSS in vivo. Consistent evidence of a robust molecular mechanism (or lack thereof) would allow clinical research to build on the epidemiological evidence and begin evaluation of PSS as supplements that could contribute to reduced global cancer burden in the prevention setting, or as treatment adjuncts that could improve prognosis for cancer patients.

Methods

Search strategy

A comprehensive search of online databases MEDLINE and Scopus was carried out throughout June 2020. Search terms are available in supplementary materials. The intention to review was submitted to PROSPERO on 9th June 2020 and was approved and published on 11th June 2020 with reference number CRD42020191337 (Thorne et al. 2020) and can be accessed at crd.york.ac.uk/PROSPERO.

Study selection

Titles and abstracts were screened for inclusion criteria; *i*) original data papers (e.g. reviews were excluded at this point); *ii*) conducted in whole organism animal models; *iii*) evaluated cancer (other diseases excluded); *iv*) phytosterol, phytostanol, a derivative/metabolite, or a mixture; *v*) English language publications; *vi*) not published in a predatory journal, listed on the website predatoryjournals.com. Screening was performed in duplicate by independent reviewers. Discrepancies were evaluated, discussed, and agreed by all members of the research team.

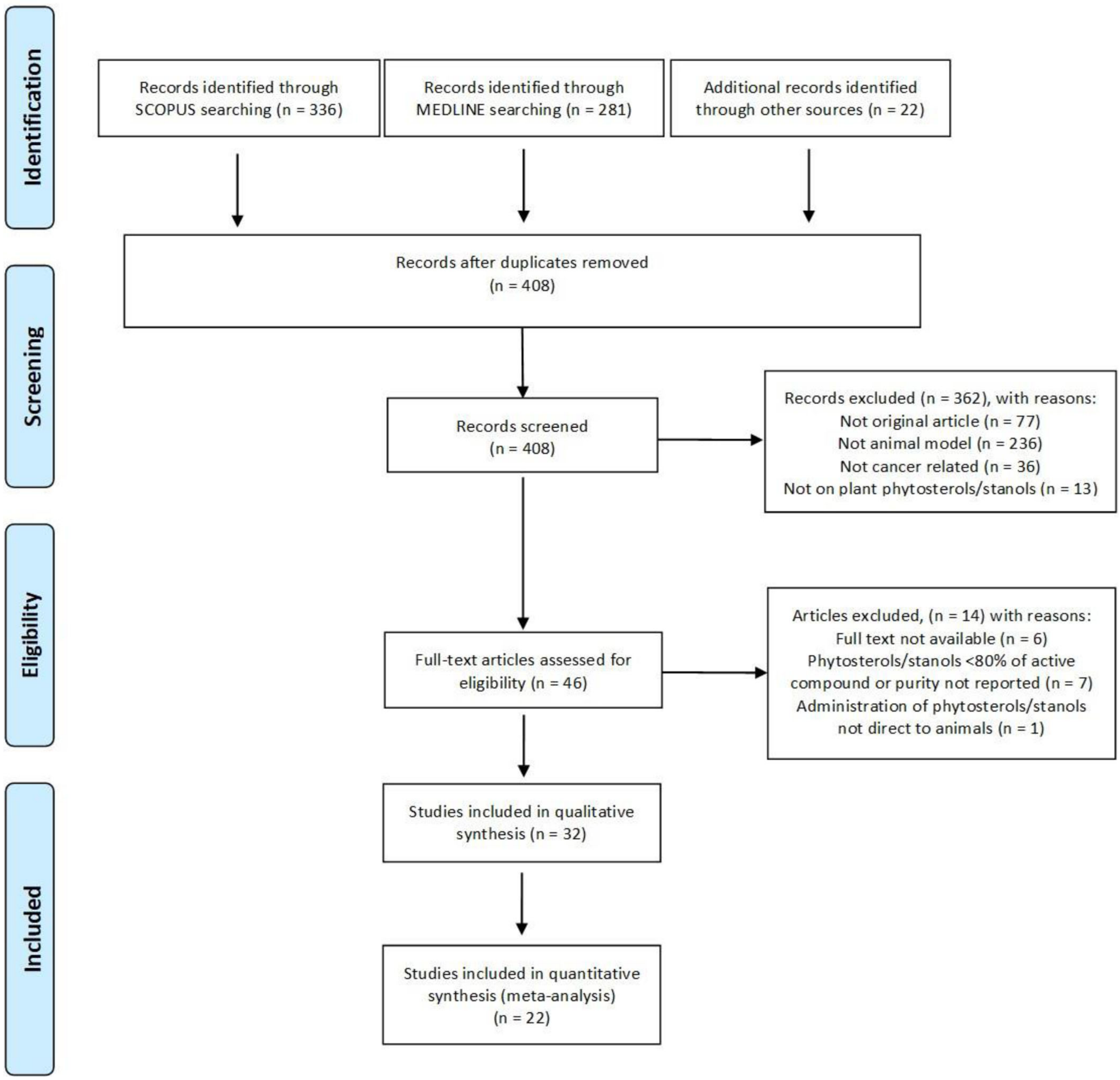

Figure 2. PRISMA flow diagram showing searching, screening, eligibility, and inclusion process.

Data extraction

All data were extracted in duplicate into Microsoft Excel by independent contributors. Any disagreements were resolved by discussion with full research team. Extracted data included information and measures on animal models; study design; intervention and control treatments, duration, and dose; cancer type; and outcome assessment. Effect sizes were extracted as means with measures of variance. Where effect sizes were only presented in figures, WebPlotDigitizer (v4.2) was used to extract data (Rohatgi 2019). Where more than 1 treatment group was compared to the same control, the effect size of the highest dose was extracted, and/or the parent PSS molecule was chosen rather than derivatives.

Statistical analysis

Meta-analyses were performed in RevMan version 5.3 (The Nordic Cochrane Centre, T. C. C 2014). Heterogeneity was anticipated between studies due to variation in animal models and treatments, so random-effects models were used if $\geq$ 3 studies were available. Where fewer than three studies were available, a fixed effects model was applied to preserve power and minimize risk of type-1 errors (Jackson and Turner 2017). In analysis where effect sizes were calculated using different metrics that could not be harmonized, standardized mean difference (SMD) was used (Borenstein et al. 2009). Effect sizes of SMD are interpreted as mean difference in units of standard deviation (versus control)

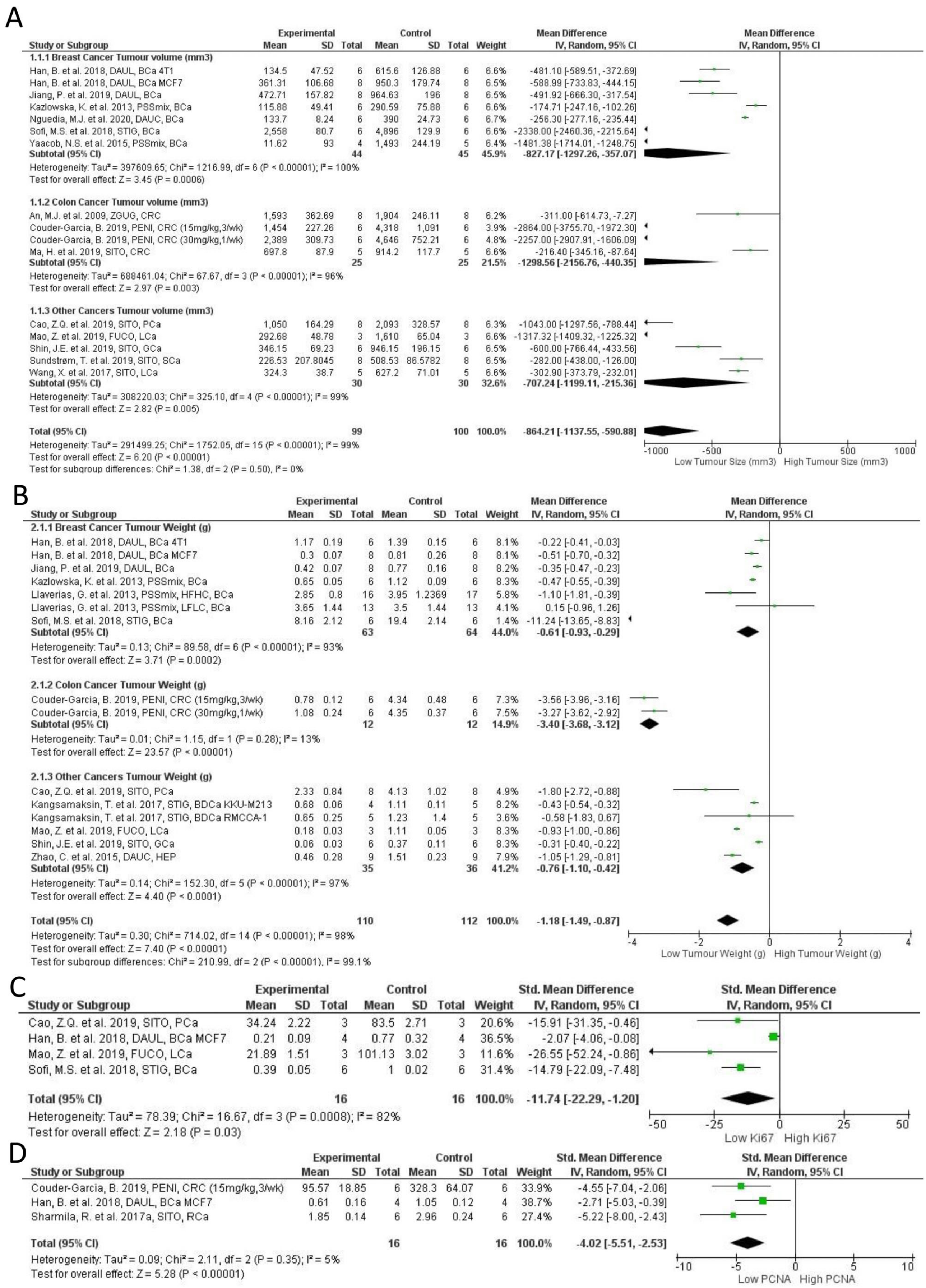

Figure 3. Forest plot of tumor size and proliferation markers after plant phytosterols and stanols administration. (A) Mean difference in change between PSS treatment and control of tumor volume (mm^3) according to cancer type. (B) Mean difference in change between PSS treatment and control of tumor weight (g) according to cancer type. (C) Standard mean difference in change between PSS treatment and control of PCNA proliferation marker. (D) Standard mean difference in change between PSS treatment and control of Ki67 proliferation marker.

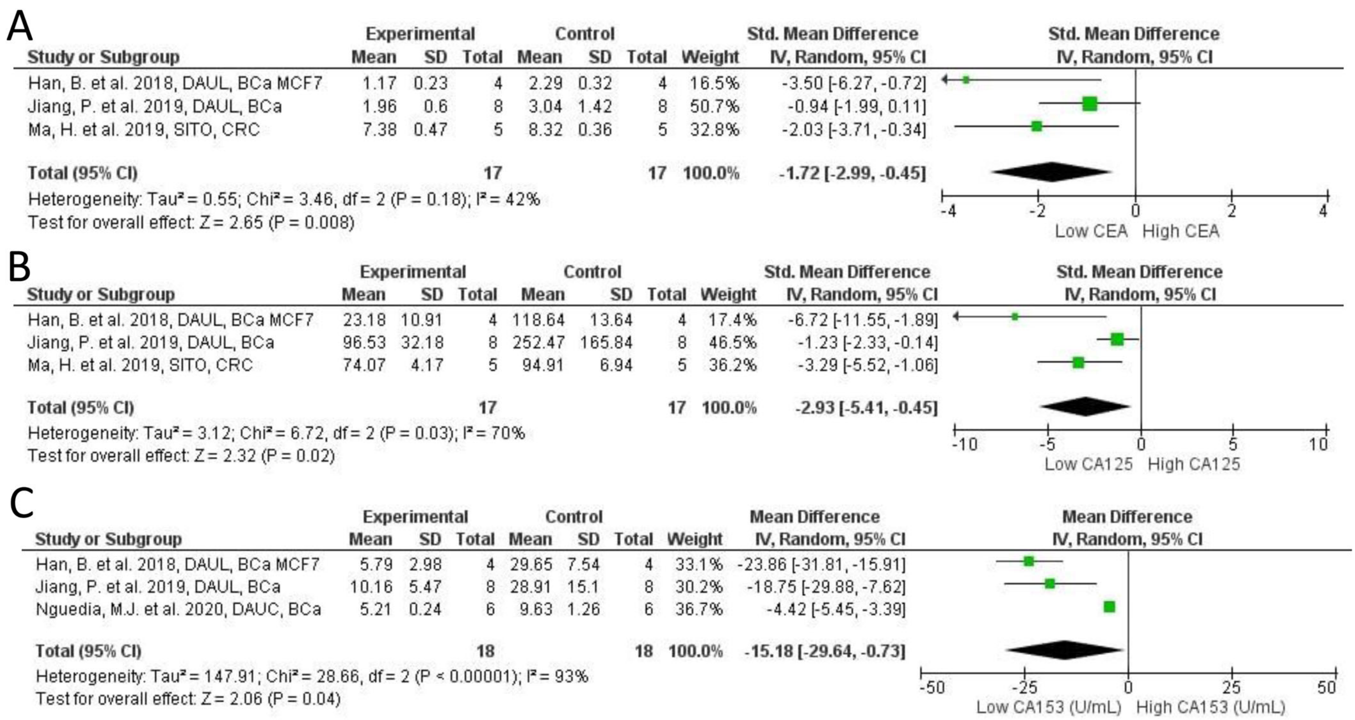

Figure 4. Forest plot of cancer serum biomarkers after plant phytosterols and stanols administration. (A) Standard mean difference in change between PSS treatment and control of CEA. (B) Standard mean difference in change between PSS treatment and control of CA125. (C) Mean difference in change between PSS treatment and control of CA153.

following exposure to the intervention. Degree of heterogeneity of meta-analyses was quantified using I^2. We anticipated that meta-analyses of animal studies would reflect higher levels of heterogeneity than human clinical trials (Vesterinen et al. 2014) as clinical trials aim to minimise inter-population variables, whereas animal studies generally aim to minimize *intra*-study variation through the use of inbred strains, strict protocol, and controlled environments. This in turn, makes the collective assessment of animal studies susceptible to high *inter*-study variation because each study has adapted its own protocol. We applied $I^2 > 75\%$ as a marker of high heterogeneity for meta-analysis of animal studies (Peter et al. 2020). In meta-analyses with $\geq$10 comparisons per outcome and $I^2 > 75\%$, sources of heterogeneity were explored and discussed (Deeks et al. 2019; Peter et al. 2020). Assessment of publication bias was performed by visual inspection where $\geq$10 studies were assessed for a single outcome.

Risk of bias

Risk of bias (ROB) was performed for experimental design and adherence to BJP and PROPSERO guidelines for animal experiments (SF1A); adherence to BJP guidelines for natural products (SF1B); adherence to BJP guidelines for immunoblotting adapted to include immunohistochemistry (SF1C).

Results

Systematic search

Three hundred and thirty-six records identified in Scopus were combined with 281 from Medline and with 22 identified through other routes (e.g. preliminary literature reviews) resulting in 408 unique records after removal of duplicates. After screening for inclusion and exclusion criteria full text of 46 records was analyzed. Thirty-two were found suitable for inclusion in qualitative synthesis (summarized in Table 1) and of these 22 were appropriate for data extraction and meta-analysis. This information is summarized in the PRISMA diagram (Figure 2).

Animal models

Mice or rats were used in all studies except for one that used zebrafish. Of the 32 studies using mammalian models, 18 employed xenograft assays, 10 induced tumors through mutagen, and 4 were spontaneous genetic cancer models. A total of nine studies evaluated colorectal cancer (CRC), 9 breast cancer (BCa), 4 skin/melanoma, 2 lung (LCa). Gastric cancer (GCa), Ehrlich-Lettre ascites carcinoma (ECa), hepatoma (HEP), cholangiocarcinoma (CCA), ovarian cancer (OCa), pancreatic cancer (PaCa), renal cancer (RCa), and prostate cancer (PCa) were each studied once. Metastasis was evaluated in three studies. Twice in the context of skin evaluating metastasis to the brain and lung, and once in breast cancer evaluating metastasis to the lung.

PSS administration

The most commonly studied PSS was sitosterol ([SITO] n = 11) and its derivatives (n = 7). Stigmasterol ([STIG] n = 4), fucosterol ([FUCO] n = 2) and PSS mixtures (n = 6) were next most common, with peniocerol (PENI) and Z-guggulsterone (ZGUG) reported once each. Campesterol

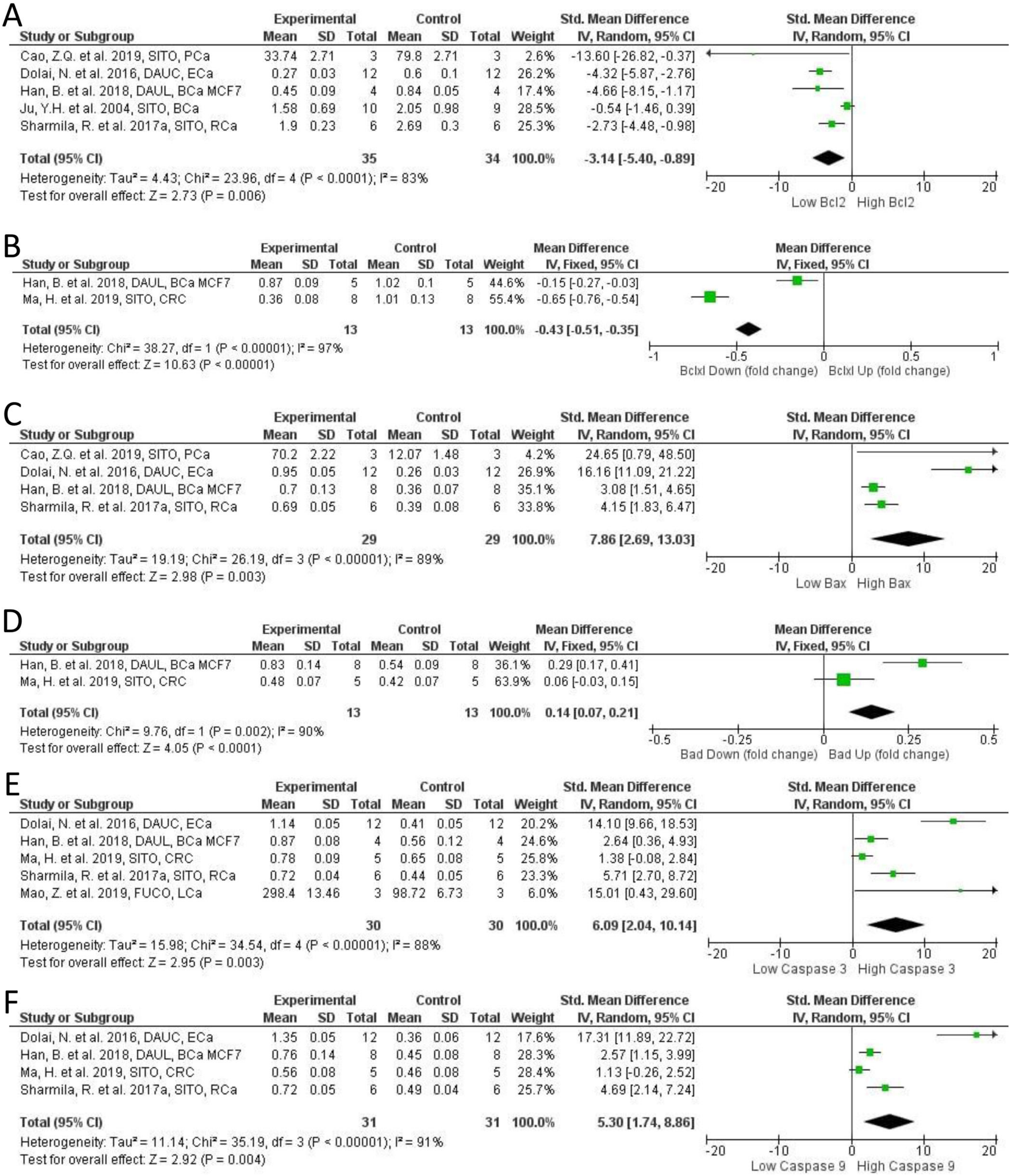

Figure 5. Forest plot of apoptosis markers after plant phytosterols and stanols administration. (A) Standard mean difference in change between PSS treatment and control of Bcl-2. (B) Mean difference in change between PSS treatment and control of Bclxl. (C) Standard mean difference in change between PSS treatment and control of Bax. (D) Mean difference in change between PSS treatment and control of Bad. (E) Standard mean difference in change between PSS treatment and control of Caspase-3. (F) Standard mean difference in change between PSS treatment and control of Caspase-9.

(CAMP), a relatively common PSS was only studied as part of PSS mixtures (n = 5). Phytostanols were only assessed as mixtures. PSS were administered via three main routes, either integrated into chow per oral (PO) (n = 15), oral gavage (OG) (n = 5), or injection intravenously (IV) (n = 1), or intraperitoneally (IP) (n = 10) or as microinjection (n = 1). The concentration of PSS to which animals were exposed varied by several orders of magnitude. Doses, normalized for a typical 65–75 kg human, ranged from the equivalent of 3 mg per person per week up to 75 g per person per day.

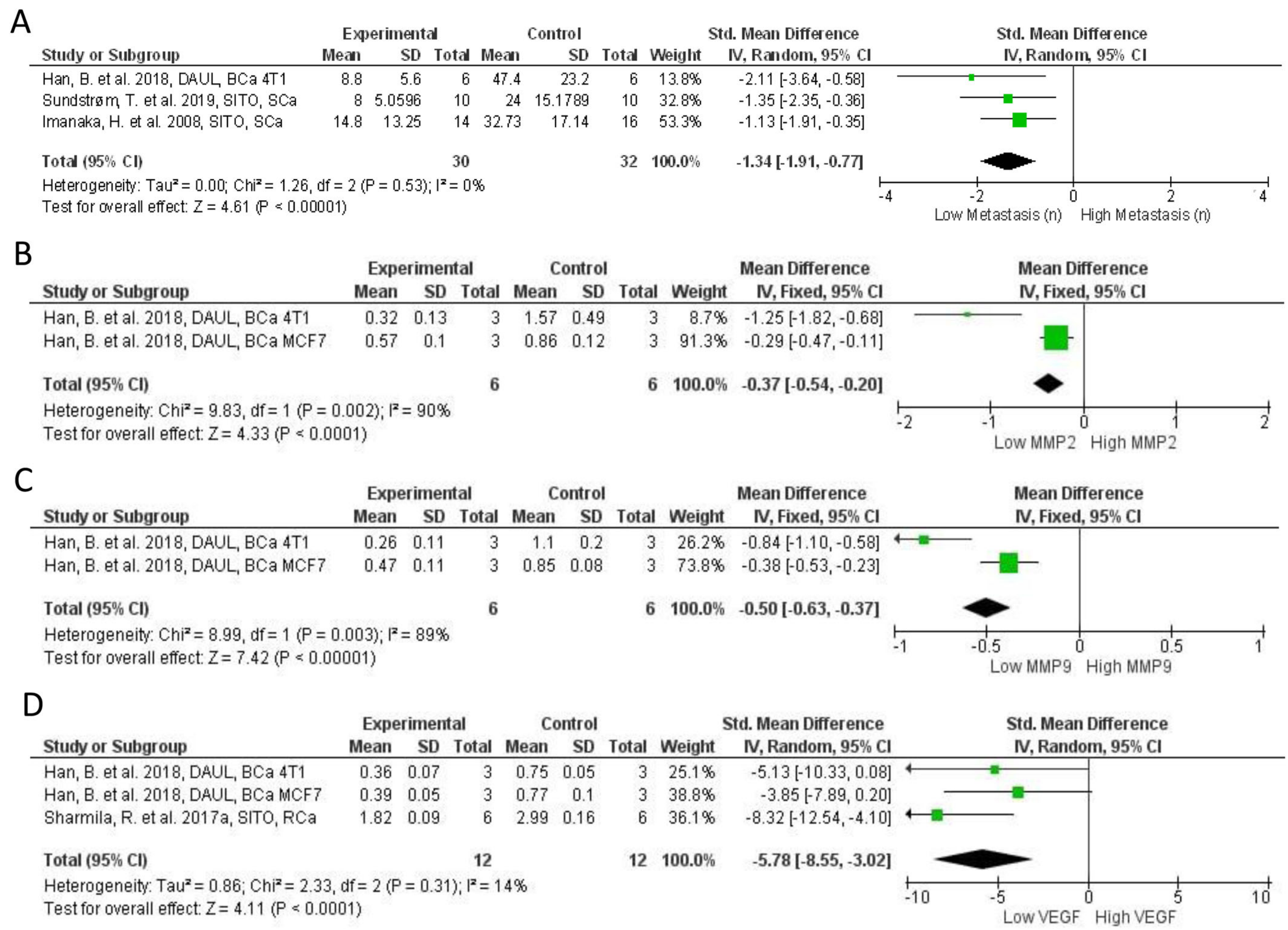

Figure 6. Forest plot of metastasis and metastasis markers after plant phytosterols and stanols administration. (A) Mean difference in change between PSS treatment and control of metastasis number. (B) Mean difference in change between PSS treatment and control of MMP2. (C) Mean difference in change between PSS treatment and control of MMP9. (D) Standard mean difference in change between PSS treatment and control of VEGF.

Sustaining proliferative signaling

A range of growth factors and signaling pathways regulate the cell cycle machinery. Typically, tumor proliferative index in humans can be measured by expression of cell cycle machinery proteins such as Ki67, PCNA, and CDKs. These proteins can be measured in tumor tissue by immunohistochemistry or immunoblotting, and tumor growth can be tracked non-invasively with calipers or measuring expression of light producing transgenes. Cells can also be isolated from tumors and flow sorted based on DNA content providing a measure of cell cycle kinetics in the tumor.

In our meta-analysis of 14 studies (16 comparisons; n = 199) across PSS treatments we report that PSS mitigates tumor growth volume in breast (MD = −827.17 mm^3; 95% CI: −1297.26, −357.07; I2 = 100%; $p < 0.001$), colon (MD = −1,298.56 mm^3; 95% CI: −2,156.76, −440.35; I2 = 96%; $p = 0.003$), other cancers (MD = −864.21 mm^3; 95% CI: −1199.11, −215.36; I2 = 99%; $p = 0.005$), and overall cancer (MD = −864.21 mm^3; 95% CI: −1137.55, −590.88; I2 = 99%; $p < 0.001$), compared to controls (Figure 3A). Similarly, tumor mass was much smaller across PSS treatments in 11 studies (15 comparisons; n = 222) reporting on breast (MD = −0.61 g; 95% CI: −0.93, −0.29; I2 = 93%; $p < 0.001$), colon (MD = −3.40 g; 95% CI: −3.68, −3.12; I2 = 13%; $p < 0.001$), other cancers (MD = −0.76 g; 95% CI: −1.10, −0.42; I2 = 97%; $p < 0.001$), and overall cancer (MD = −1.18; 95% CI: −1.49, −0.87; I2 = 98%; $p < 0.001$), compared to controls (Figure 3B). For overall total cancer mass (Figure 3A) and volume (Figure 3B), we observed very high heterogeneity (I^2>75%) which is likely attributed to differences in effect sizes between cancer models. No evidence of publication bias was observed in funnel plots for either analyses (data not shown). Tumor growth was also assessed in several studies via plasma markers CEA, CA125, and CA153. All markers were significantly reduced in PSS groups compared to controls (Figure 4A–C).

Deregulation of signaling pathways can lead to structural changes in epithelial cell organization leading to formation of aberrant crypt foci (ACF), an early marker of CRC risk (Alrawi et al. 2006). SITO at a range of doses between 5 and 20 mg/kg per day (Baskar et al. 2010), and at 0.2% dw PO (Deschner et al. 1982) reduced colonic epithelial cell proliferation, ACF and crypt multiplicity, as well as tumor growth in xenograft CRC. In a DMBA mutagen model of skin cancer, STIG (0.2–0.4 g/kg PO) resulted in fewer and smaller skin papillomas, which were preceded by significantly longer latency period (Ali et al.

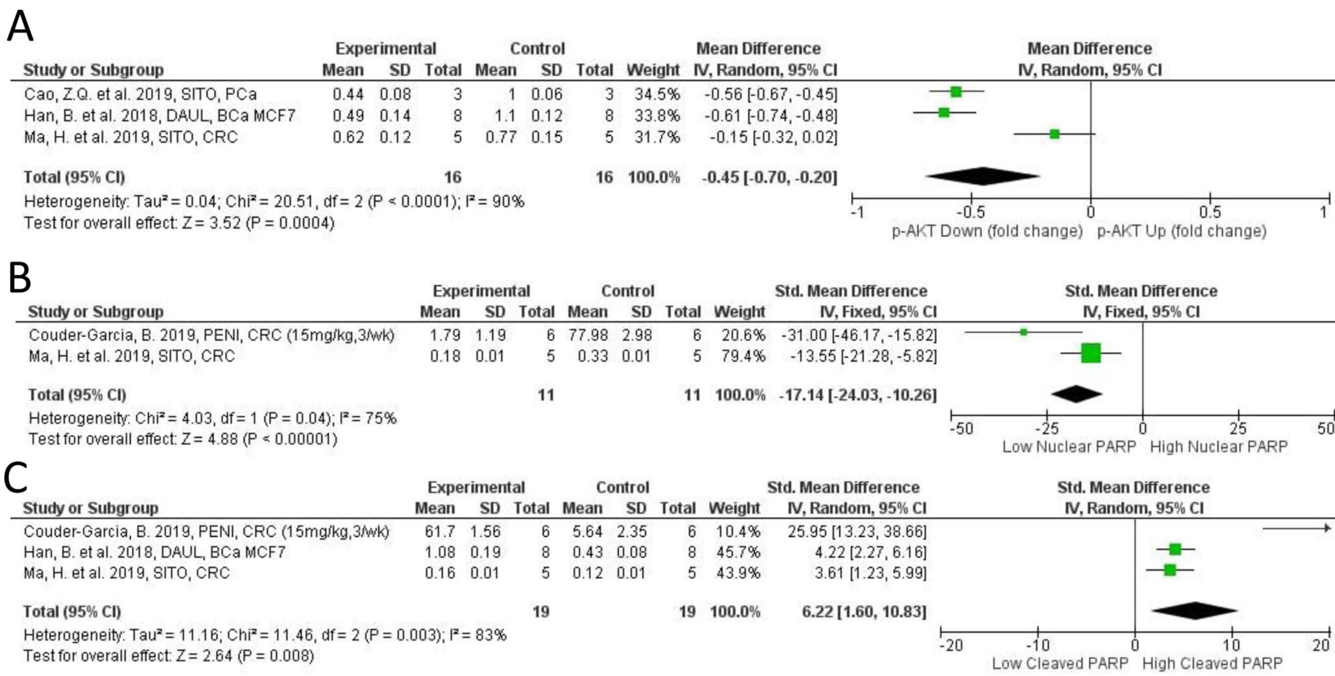

Figure 7. Forest plot of pAKT and PARP expression after plant phytosterols and stanols administration. (A) Standard mean difference in change between PSS treatment and control of pAKT. (B) Standard mean difference in change between PSS treatment and control of nuclear PARP. (C) Mean difference in change between PSS treatment and control cleaved PARP.

2015). STIG (50 mg/kg IP) also slowed tumor cell doubling time in a melanoma xenograft model (Iyer and Patil 2012). Yaccob and colleagues found a striking reduction in an NMU mutagen model of breast cancer, where tumor number was reduced 10-fold suggesting that induced tumors actually regressed in the treatment group (Yaacob et al. 2015).

Expression of cell proliferation markers such as Ki67, PCNA, components of the cell cycle machinery, and proliferation promoting oncogenes were evaluated in several studies. When amalgamated we found a significant reduction in Ki67 (SMD = −11.74; 95% CI: −22.29, −1.20; $p = 0.03$; Figure 3C) and PCNA (SMD = −4.02; 95% CI: −5.51, −2.53; $p < 0.0001$; Figure 3D). Ki67 was evaluated by western Blot (WB) or immunohistochemistry (IHC) in four studies, investigating 20, 40, 60, 80, 100 mg/kg treatments. Ki67 and PCNA were significantly reduced across all studies. Interestingly, Ki67 was reduced by FUCO in LCa in a convincing dose-dependent manner (Mao et al. 2019) as was PCNA by PENI dose (15 mg or 30 mg/kg weekly) and frequency (15 mg/kg once/week or three/week) in CRC xenograft HCT116 (Couder-García et al. 2019). Aside from Ki67 and PCNA, Cyclin D1, a proliferation control protein, was reduced by 50% in the tumors of SITO treated KCa models (Sharmila and Sindhu 2017a), but was unchanged in another study where very high PSS containing chow was provided to Apc^{min} mice (Marttinen et al. 2014) (Table 1).

A range of studies have considered tumor cell proliferation after exposing models to PSS mixtures, which are arguably more representative of typical human exposure. In physiological doses PSS mixtures exerted their inhibitory effects on tumor growth in different cancer types like cholangiocarcinoma and breast cancer (Kangsamaksin et al. 2017; Kazłowska et al. 2013). In an N-Nitroso-N-methylurea (MNU) carcinogen induced model of CRC, mice were fed with different doses of PSS in feed (0.3%, 1% and 2% dw) of a PSS mixture (60% SITO, 30% CAMP, 5% STIG) preneoplastic lesion formation was reduced (Janezic and Rao 1992). Ju et al. evaluated exposure to very high doses of a PSS mixture (9.8 g/kg SITO+ 0.2 g/kg STIG) in chow and observed reduced tumor area in BCa xenograft mouse (Ju et al. 2004), and Yaacob who applied somewhat lower doses (40 mg/kg: 53% SITO, 16% CAMP, 26% STIG) also found reduced tumor volume and number in an MNU mutagen model of BCa (Yaacob et al. 2015).

At cancer sites where exposure to dietary compounds is considered highest, such as the GI tract, some studies found PSS mixtures to not be so effective. Rats fed with 24 mg/rat/day of a PSS mixture (55% SITO, 41% CAMP, 4% STIG) developed a similar tumor burden to their controls and were likely to suffer complications from poor gut bacterial health (Quilliot et al. 2001). Notably, CAMP made up a large proportion of this PSS mixture. A phytosterol mixture again containing high CAMP, provided at exceptionally high levels via chow (20 mg/mouse/day, which when calculated by weight by weight, is equivalent to 70 g/person/day), was found to promote tumor formation in the Apc^{min} mouse model (Marttinen et al. 2014). In an experimentally matched study by the same group, the same dose of phytostanols was also found to promote tumor formation in the same model (Marttinen et al. 2013).

Combined, the broad consensus in the published data indicates that PSS is anti-proliferative in vivo, and reduced tumor growth is associated with lower expression of proliferation markers such as Ki67 and PCNA. However, in some studies performed at very high doses, especially in mixtures containing high CAMP or CAMS concentrations, PSS appeared to be either ineffective, led to gut health complications, or in two cases promoted tumor growth and

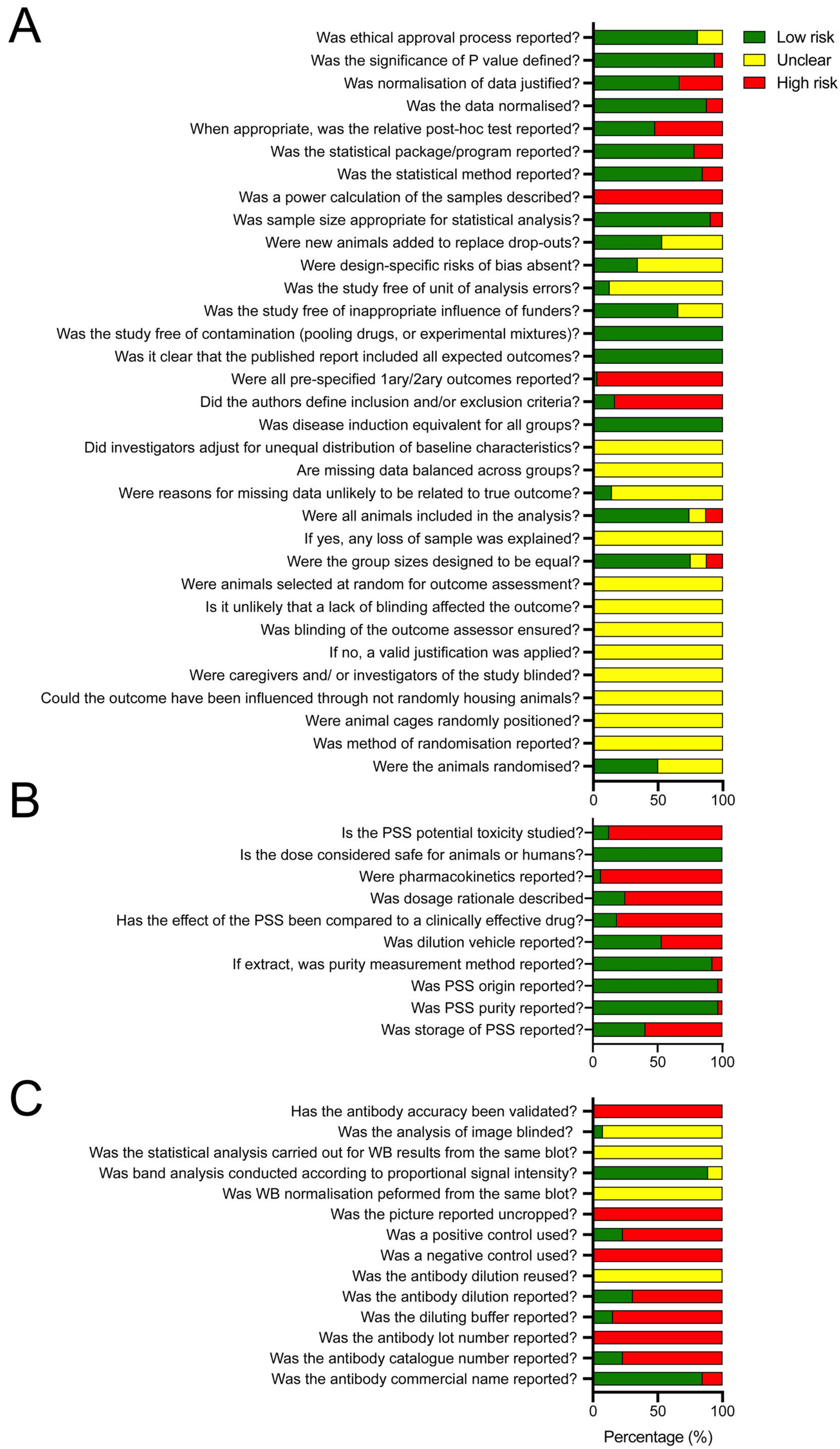

Figure 8. Risk of bias analysis and adherence scores for animal research, immunoblotting, and research on natural products.

Table 1. Summary of all extracted data.

Article	Cancer	Model gene/cell line/mutagen number	Route/frequency/ treatment time (days)	Dose, diluent	Tumor metrics	Sustaining proliferative signaling	Resisting cell death	Activating invasion and metastasis	Inducing angiogenesis	Enabling replicative immortality	Tumor-promoting inflammation	Oncogenes and tumor suppressor genes
Ali, H. et al. 2015 STIG	Skin papilloma	Mutagen: DMBA Swiss albino mice 10/group	PO, 3/week, 112	200 mg/kg Chow	Papilloma (n) × 0.4 Vol. × 0.5 Latency × 1.3	NR	NR	ALP (IU/L) × 0.5	NR	DNA damage (%tail DNA) × 0.6	SOD1 (µmole/mg/ protein) × 1.1 CAT (U/mg/protein) × 3.2 LPO (nmole/mg/ protein) x 0.5 GSH (µmole/mg/ protein) × 2.3 AST (IU/L) × 0.7 ALT (IU/L) × 0.7	NR
				400 mg/kg Chow	Papilloma (n) × 0.1 Vol. × 0.5 Latency × 1.3	NR	NR	ALP (IU/L) × 0.3	NR	DNA damage (%tail DNA) × 0.3	SOD (µmole/mg/ protein) × 1.3 CAT (U/mg/protein) × 4.4 LPO (nmole/mg/ protein) 0.6 GSH (µmole/mg/ protein) × 3.4 AST (IU/L) × 0.6 ALT (IU/L) × 0.5	NR
An et al. 2009	Colon	Xenograft: HT29	IP, daily, 14	20 mg/ kg DMSO	Vol. × 0.4	NR	NR	NR	NR	NR	NR	NR
GUGG		nu/nu mice 6/group		40 mg/ kg DMSO	Vol. × 0.2	NR	NR	NR	NR	NR	NR	NR
Awad A.B. et al. 2001 56% SITO, 28% CAMP, 10% STIG	Prostate	Xenograft: PC3 C.B.-17 SCID mice 8-12/ group	PO, 70, daily	2% dw Chow	Area × 0.7	NR	NR	Animals developed metastasis (n) × 0.4 Animals with lung metastasis (n) × 0.4 Animals with liver metastasis (n) × 0 Animals with lymph nodes metastasis (n) × 0.7	NR	NR	NR	NR
Bae et al. 2020 FUCO	Ovarian	Xenograft: ES2	MI, once, 1	40µM DMSO	Tumor formation (RFI %) × 0.8	NR	NR	NR	NR	NR	NR	NR
		Zebrafish		60µM DMSO	Tumor formation (RFI %) × 0.6	NR	NR	NR	NR	NR	NR	NR
		10/group		100µM, DMSO	Tumor formation (RFI %) × 0.4	NR	NR	NR	NR	NR	NR	NR
		Xenograft: OV90		40µM, DMSO	Tumor formation (RFI %) × 0.7	NR	NR	NR	NR	NR	NR	NR
		Zebrafish		60µM, DMSO	Tumor formation (RFI %) × 0.5	NR	NR	NR	NR	NR	NR	NR
		10/group		100µM, DMSO	Tumor formation (RFI %) × 0.4	NR	NR	NR	NR	NR	NR	NR
Baskar et al. 2010, SITO	Colon	Mutagen: DMH Albino Wistar rats 6/group	PO, daily, 112	5 mg/ kg, CMC	ACF (n) NS AC (n) × 0.8 AC/ACF (n) × 0.9 %ACF inhibition × 0.4	NR	NR	NR	NR	NR	NR	NR
				10 mg/ kg, CMC	ACF (n) × 0.7 AC (n) × 0.6 AC/ACF (n) × 0.8 %ACF inhibition × 0.5	NR	NR	NR	NR	NR	NR	NR
				20 mg/ kg, CMC	ACF (n) × 0.6 AC (n) × 0.4	NR	NR	NR	NR	NR	NR	NR

					AC/ACF (n) × 0.6 %ACF inhibition × 0.7							
Cao, Z.Q. et al. 2018 SITO	Pancreatic	Xenograft: BXPC-3 BALB/c mice (nu/nu) 8 per group	IP, daily, 28	80 mg/kg, DMSO	Vol. × 0.5 Wei. × 0.6	Ki67 (% × 0.4	Bax/Bcl2 × 5.0 Bax × 5.8 Bcl2 × 0.4	Vimentin × 0.3 E cadherin × 2.2 Snail × 0.3	NR	NR	NR	pNFκB/NFκB × 0.3 pAkt/Akt × 0.4 GSK3β/pGSK3β × 0.7 pGSK (%)× 0.5
Couder-Garcia, B.D.C. et al. 2019 PENI	Colon	Xenograft: HCT116 nu/nu mice 6/group	IP, 1/week, 21	15 mg/kg, sesame oil and 5% DMSO	Vol. × 0.6 Wei. × 0.2	PCNA × 0.4	NR	NR	NR	NR	NR	Nuclear PARP1 × 0.05 Cleaved PARP1 × 9.7
				30 mg/kg, sesame oil and 5% DMSO	Vol. × 0.5 Wei. × 0.2	PCNA × 0.5	NR	NR	NR	NR	NR	Nuclear PARP1 × 0.03 Cleaved PARP1 × 10.6
			IP, 3/week, 21	15 mg/kg, sesame oil and 5% DMSO	Vol. × 0.3 Wei. × 0.2	PCNA × 0.3	NR	NR	NR	NR	NR	Nuclear PARP1 × 0.03 Cleaved PARP1 × 10.9
Deshner, E.E. et al. 1982 SITO	Colon	Mutagen: MNU Fischer rats, 6/control, 8/treatment	PO, daily, 196	0.2% dw, Chow	Colonic epithelial cell proliferation NS	NR	NR	NR	NR	NR	NR	NR
Dolai et al. 2016 DAUC	Ehrlich-Lettre ascites carcinoma	Xenograft: EAC cells treated mice Swiss albino mice 12/ group	IP, daily, 14	50 mg/kg, NR	NR	NR	Bcl2 × 0.7 Bax × 2.8 Bcl2/Bax × 0.7 Casp3 × 2.2 Casp9 × 3.1 apoptotic cells 35.3% increase	NR	NR	NR	NR	p53 × 1.3 p21 × 2.6
				100 mg/kg, NR	NR	NR	Bcl2 × 0.5 Bax × 3.7 Bcl2/Bax × 0.6 Casp3 × 2.8 Casp9 × 3.8 apoptotic cells 38.6% increase	NR	NR	NR	NR	p53 × 1.7 p21 × 3.4
Han, B. et al. 2018 DAUL	Breast	Xenograft: MCF-7 BALB/c nude mice 3-8/group	OG, daily, 29	25 mg/kg, distilled water (1% Tween 80)	Vol. NS Wei. NS	CEA (ng/ml) NS CA125 (IU/ml) NS CA153 (IU/ml) × 0.7	Casp3 NS Casp9 NS Bad × 1.6 Casp7 NS Casp8 × 4.3 Bclxl × 0.7 Bax NS XIAP × 0.5 Bcl2 × 0.6	MMP2 NS MMP9 NS	VEGF NS	NR	NR	Cleaved PARP1 NS NFκB (ng/ml) NS PI3K NS AKT NS pAKT NS IKKα/B NS pIKKα/B NS IkBα NS pIkBα NS p65 NS pP65 NS
				50 mg/kg, distilled water (1% Tween 80)	Vol. × 0.8 Wei. × 0.7	CEA (ng/ml) × 0.5 CA125 (IU/ml) × 0.6 CA153 (IU/ml) × 0.5	Casp3 × 1.4 Casp9 × 1.4 Bad × 1.5	MMP2 × 0.7 MMP9 × 0.7	VEGF NS	NR	NR	Cleaved PARP1 × 1.8 NFκB(ng/ml) × 0.6

(*continued*)

Table 1. Continued.

Article	Cancer	Model gene/cell line/mutagen number	Route/frequency/treatment time (days)	Dose, diluent	Tumor metrics	Sustaining proliferative signaling	Resisting cell death	Activating invasion and metastasis	Inducing angiogenesis	Enabling replicative immortality	Tumor-promoting inflammation	Oncogenes and tumor suppressor genes
							Casp7 NS Casp8 × 4.3 Bclxl × 0.6 Bax × 2 XIAP × 0.4 Bcl2 × 0.4					PI3K NS AKT NS pAKT × 0.8 IKKα/B NS pIKKα/B × 0.5 IkBα NS pIkBα × 0.9 P65 NS pP65 × 0.7
				100 mg/kg, distilled water (1% Tween 80)	Vol. × 0.4 Wei. × 0.4	CEA (ng/ml) × 0.5 CA125 (IU/ml) × 0.2 CA153 (IU/ml) × 0.2 PCNA × 0.6 Ki67 × 0.3	Casp3 × 1.5 Casp9 × 1.7 Bad × 1.5 Casp7 × 0.7 Casp8 × 4.3 Bclxl × 0.4 Bax × 1.9 XIAP × 0.4 Bcl2 × 0.5	MMP2 × 0.7 MMP9 × 0.5	VEGF × 0.5	NR	NR	Cleaved PARP1 × 2.5 NFκB (ng/ml) × 0.5 PI3K × 0.7 AKT NS pAKT × 0.4 IKKα/B NS pIKKα/B × 0.3 IkBα NS pIkBα × 0.4 P65 × 0.3 pP65 × 0.4
		Xenograft: luciferase expressing 4T1 BALB/c nude mice 6/group	OG, daily, 23	100 mg/kg, distilled water (1% Tween 80)	Vol. NS Wei. NS	NR	NR	MMP2 × 0.2 MMP9 × 0.2 Lung met. by luciferase × 0.2 Lung met. by nodules (n) × 0.2	VEGF × 0.5	NR	NR	NR
Iyer, D. et al. 2012 STIG	Melanoma	Xenograft: B16F1 C57BL6 strain + Swiss albino strain 6/group	IP, daily, 10	50 mg/kg, distilled water and Tween 80)	Vol. doubling time (VDT) × 3	NR	NR	NR	NR	NR	NR	NR
Imanaka, H. et al. 2008 SITO (liposomal)	Melanoma	Xenograft, B16BL6 C57BL/6 mice 14/treatmen,16/control	PO, daily, 7	4 mmol as sterols/mouse liposomes	NR	NR	NR	colonies (n) metastasis × 0.5	NR	NR	NR	NR
Janezic, S.A. et al. 1992 PSS mixture (60% SITO, 30% CAMP, 5% STIG)	Colon	Mutagen: MNU C57B1/6J mice 6/group	PO, daily, 14	0.3% dw, Chow	Labelling Index (%) NS Cell position × 0.8 Miotic index (%) × 0.5	NR	NR	NR	NR	NR	NR	NR
				1% dw, Chow	Labelling Index (%) × 0.7 Cell position × 0.5 Mitotic index (%) × 0.5	NR	NR	NR	NR	NR	NR	NR
				2% dw, Chow	Labelling Index (%) × 0.4 Cell position × 0.4 Mitotic index (%) × 0.4	NR	NR	NR	NR	NR	NR	NR
Jiang et al. 2019 DAUN	Breast	Xenograft: MCF-7 BALB/c nude mice	PO, daily, 28	87.8 mg/kg/	Vol. × 0.4 Wei. × 0.4	CEA (ng/ml) × 0.5 CA125 (IU/ml) × 0.4	NR	NR	NR	NR	NR	NR

DAUL		8/group		mouse, distilled water containing 1% Tween 80 87.8 mg/kg/ mouse, distilled water containing 1% Tween 80	Vol. × 0.5 Wei. × 0.5	CA153 (U/mL) × 0.3 CEA (ng/ml) × 0.6 CA125 (IU/ml) × 0.4	NR	NR	NR	NR	NR	NR
DAUP				87.8 mg/kg/ mouse, distilled water containing 1% Tween 80	Vol. × 0.4 Wei. × 0.4	CA153 (U/mL) × 0.4 CEA (ng/ml) × 0.6 CA125 (IU/ml) × 0.4 CA153 (U/mL) × 0.1	NR	NR	NR	NR	NR	NR
Ju, Y.H. et al. 2004 SITO	Breast	Xenograft: MCF-7 BALB/c (nude) mice	PO, daily, 77	9.8 g/kg dw, Chow	Area × 0.8	NR	Bcl2 NS	NR	NR	NR	NR	NR
DAUC		9-10/group		0.2 g/kg dw, Chow	Area NS	NR	Bcl2 NS	NR	NR	NR	NR	NR
Kangsamaksin, T. et al. 2017 STIG		Xenograft: KKU-M213 C57BL/6 mice	OG, 3/week, 28	10 mg/kg, NR	Wei. × 0.6	NR	NR	NR	CD31 (IHC) × 0.6	NR	NR	NR
		5/group Xenograft: RMCCA-1 C57BL/6 mice			Wei. × 0.5	NR	NR	NR	NR	NR	NR	NR
	Cholangiocarcinoma	5/group Xenograft: KKU-M213 C57BL/6 mice			Wei. × 0.7	NR	NR	NR	CD31 (IHC) × 0.6	NR	NR	NR
LUPE		5/group Xenograft: RMCCA-1 C57BL/6 mice			Wei. × 0.5	NR	NR	NR	NR	NR	NR	NR
		5 per group Xenograft: KKU-M213 C57BL/6 mice		10 mg/kg STIG + 10 mg/kg LUP, NR	Wei. × 0.4	NR	NR	NR	CD31 (IHC) × 0.5	NR	NR	NR
50% STIG, 50% LUPE		6 per group Xenograft: RMCCA-1 C57BL/6 mice			Wei. × 0.2	NR	NR	NR	NR	NR	NR	NR
Kazlowska, K. et al. 2013	Breast	6 per group Xenograft: 4T1 BALB/c mice	IP, every 3 days, 18	5 mg/kg, NR	Vol. NS	NR	NR	NR	NR	NR	NR	NR
PSS mixture (55% SITO, 30% CAMP)		6/group		10 mg/kg, NR	Vol. × 0.5 Wei. × 0.7	NR	NR	NR	NR	NR	NR	NR
				25 mg/kg, NR	Vol. × 0.4 Wei. × 0.6	NR	NR	NR	NR	NR	NR	NR
Llaverias, G. et al. 2013 LFLC 41% SITO, 22% STIG, 20% CAMP	Breast	Genetic: transforming oncogene PyMT antigen MMTV-PyMT Tg mice	PO, daily, 56-91	Chow	Area. NS Wei. NS	NR	NR	NR	NR	NR	NR	NR
HFHC 41% SITO, 22% STIG, 20% CAMP		7-16/group		Chow	Area. × 0.5 Wei. × 0.7	NR	NR	NR	n of CD31 positive microvessels / normal tissue field NS n of CD31 positive microvessels / hyperplasia tissue field NS n of CD31 positive microvessels / adenoma tissue field NS n of CD31 positive microvessels / carcinoma tissue field NS	NR	NR	NFκB × 0.6
Ma, H. et al. 2019 SITO	Colon	Xenograft: HCT116 BALB/c nude mice 5/group	OG, daily, 30	60 mg/kg, NR	Vol. × 0.8	CEA (U/ml) × 0.9 CA125 (U/ml) × 0.8 CA199 (U/mL) NS CA242 (U/mL) × 0.7	Casp9 NS Casp3 NS Casp9 (IHC) × 1.5 Casp3 (IHC) NS Cyto-C NS	NR	NR	NR	NR	Nuclear PARP × 0.5 Cleaved PARP × 1.3 pPI3K NS pAKT (ser473) NS

(continued)

Table 1. Continued.

Article	Cancer	Model gene/cell line/mutagen number	Route/frequency/ treatment time (days)	Dose, diluent	Tumor metrics	Sustaining proliferative signaling	Resisting cell death	Activating invasion and metastasis	Inducing angiogenesis	Enabling replicative immortality	Tumor-promoting inflammation	Oncogenes and tumor suppressor genes
DAUC				60 mg/ kg, NR	Vol. × 0.6	CEA (U/ml) × 0.8 CA125 (U/ml) × 0.7 CA199 (U/mL) × 0.8 CA242 (U/mL) × 0.5	Bclxl NS Bad NS Casp9 × 1.6 Casp3 × 1.5 Casp9 IHC × 2.3 Casp3 IHC × 1.4 CytoC × 1.4 BCLXL × 0.7	NR	NR	NR	NR	Nuclear PARP × 0.3 Cleaved PARP × 2.4 pPI3K × 0.7 pAKT (ser473) × 0.6
DAUL				60 mg/ kg, NR	Vol. × 0.4	CEA (U/ml) × 0.6 CA125 (U/ml) × 0.5 CA199 (U/mL) × 0.6 CA242 (U/mL) × 0.4	BAD × 1.4 Casp9 × 1.7 Casp3 × 1.8 Casp9 (IHC) × 2.8 Casp3 (IHC) × 1.8 CytoC × 1.9 Bclxl × 0.4	NR	NR	NR	NR	Nuclear PARP × 0.2 Cleaved PARP × 3.6 pPI3K × 0.3 pAKT (ser473) × 0.4
Mao, Z. et al. 2019 FUCO	Lung	Xenograft: A549 C57BL/6 mice *n* NR	IP, 3/week, 42	20 mg/ kg, Saline	Vol. × 0.7 Wei. × 0.6	Ki67 × 0.6	Bad × 1.6 Casp3 (IHC) × 1.6	NR	NR	NR	NR	NR
				40 mg/ kg, Saline	Vol. × 4. Wei. × 0.3	Ki6 × 0.4	Casp3 (IHC) × 2.3	NR	NR	NR	NR	NR
				80 mg/ kg, Saline	Vol. × 0.2 Wei. × 0.2	Ki6 × 0.2	Casp3 (IHC) × 3.0	NR	NR	NR	NR	NR
Marttinen, M. et al. 2013. (a) PSS mixture 0.8% (w/w) CAMS and STAN	Colon	Genetic: *Apc*[Min] C57BL/6J *Apc*[Min]/+ mice 14/group	PO, daily, 63	0.8 mg/ 100g diet, Chow	$n \times 2.2$	pEGFR × 1.7 EGFR × 5.5 Cyclin D1 NS pERK1/2 × 2.5	NR	NR	NR	NR	NR	NR
Marttinen, M. et al. 2013. (b) PSS mixture 0.8% (w/w) including CAMP and SITO	Colon	Genetic: *Apc*[Min] C57BL/6J *Apc*[Min]/+ Male mice 5-7/group	PO, daily, 63	0.8 mg/ 100g diet, Chow	NR	Nuclear Cyclin D1 NS EGFR NS pEGFR NS ERK1/2 NS pERK NS ERα NS ERβ NS	NR	NR	NR	NR	NR	Membrane β catenin NS Cytosol β catenin NS Nuclear β catenin NS Membrane Cav1 NS
		Genetic: *Apc*[Min] C57BL/6J *Apc*[Min]/+ Female mice 5-7/group			NR	Nuclear Cyclin D1 NS EGFR NS pEGFR NS ERK1/2 NS pERK NS ERα NS ERβ NS	NR	NR	NR	NR	NR	Membrane β catenin NS Cytosol β catenin NS Nuclear β catenin NS Membrane Cav1 NS
Nguedia, M.Y. et al. 2020 DAUC	Breast	Mutagen: DMBA Wistar rats 6/group	OG, daily 28	2.5 mg/kg, 2% ethanol	Vol. × 0.6	CA153 (U/mL) NS	NR	NR	NR	NR	SOD1 (u/mg/protein) NS CAT (mM H_2O_2/min/ mg/ protein) NS	NR

				5 mg/ kg, 2% ethanol	Vol. × 0.3	CA153 (U/mL) × 0.6	NR	NR	NR	NR	MDA (mM/mg protein) × 0.8 SOD1 (u/mg/protein) NS CAT (mM H_2O_2/min/ mg/protein) × 1.4	NR
				10 mg/ kg, 2% ethanol	Vol. × 0.3	CA153 (U/mL) × 0.5	NR	NR	NR	NR	MDA (mM/mg protein) × 0.6 SOD1 (u/mg/protein) NS CAT activity (mM H_2O_2/ min/mg/protein) × 1.4 MDA (mM/mg protein) × 0.2	NR
Quilliot, D. et al. 2001 PSS mixture (41% CAMP, 55% SITO,4% STIG)	Colon	Mutagen: MNU Wistar rats 20/group	PO, daily, 210	24 mg/ rat, Chow	Tumor number/ tumor bearing animals (n) NS Tumors/animal (n) NS CGLF/ animal NS	NR	NR	NR	NR	NR	NR	NR
Sharmila and Sindhu 2017a SITO	Kidney	Mutagen: DEN-Fe-NTA Albino Wistar rats 6/group	PO, 3/week, 168	20 mg/ kg, 0.1% CMC	NR	PCNA × 0.6 Cyclin D1 × 0.5	Bax/Bcl2 × 2.3 Bax × 1.8 Bcl2 × 0.7 Casp3 × 1.6 Casp9 × 1.5	NR	VEGF × 0.6	NR	NR	NR
Sharmila and Sindhu 2017b SITO	Kidney	Mutagen: DEN-Fe-NTA Albino Wistar rats 6/group	PO, 3/week, 168	20 mg/ kg, 0.1% CMC	NR	Cjun × 0.6 Cfos × 0.6 EGFR × 0.5 pJNK × 0.5 pERK × 0.4 pP38 MAPK × 0.6	NR	NR	NR	DNA damage (% DNA in tail intensity) × 0.5 DNA damage (Tail length) × 0.4 DNA damage (Tail movement) × 0.4 DNA damage (Olive Tail Movement) × 0.4	NR	NR
Shin et al. 2018SITO	Gastric	Xenograft: AGS BALB/c mice 6/group	IV, daily, 77	100 mg/kg, NR	Vol. × 0.4 Wei. × 0.2	NR	NR	NR	NR	NR	NR	NR
Sofi et al. 2018STIG	Breast	Mutagen: DMBA Sprague Dawley rats 6/group	PO, every 4 days, 35	10 mg/ kg, Chow	Vol. × 0.5 Wei. × 0.4	Ki67 (IHC) × 0.4 GGT plasma (IU/dl) × 0.6 GGT liver (μmol/min /mg/protein) × 0.6 LDH plasma (IU/dl) × 0.5 LDH liver (μmol /min/mg/protein) × 0.6	TUNEL positivity× 34.2	ALP liver (μmol/min /mg protein) × 0.7 ALP plasma (μmol/min/mg protein) × 0.7	NR	NR	NR	NR
Sundstrøm, T. et al. 2019 SITO	Melanoma Brain Metastasis	Genetic: Prkdc^{scid}/NcrCrl NOD.CB17 mice 8-10/group	IP daily 44-56	5 mg/ kg, olive oil or saline	Vol. NS	NR	NR	Brain metastasis (MRI count) × 0.3 Brain metastasis (luminescence) × 0.2	NR	NR	NR	NR
Wang et al. 2017SITO	Lung	Xenograft: A549 NOD/SCID mice 5/group	IP every 2 days 25	1mg/ kg, NR	Vol. × 0.5	NR	NR	NR	NR	NR	NR	NR
Yaacob, N.S. et al. 2015 PSS mixture (53% SITO, 16% CAMP, 26% STIG)	Breast	Mutagen: MNU Sprague Dawley rats 4 treatment, 5/control	OG daily 56	40mg/ kg NR	Vol. × 0.008 n × 0.1	NR	NR	NR	NR	NR	NR	NR
Zhao et al. 2015DAUC	Hepatoma	Xenograft: H22 ICR mice 9-10/group	PO daily, 7	0.5 mg/kg, DMSO	Wei. × 0.5	NR	NR	NR	NR	NR	NR	NR
				2.5 mg/kg, DMSO	Wei. × 0.3	NR	NR	NR	NR	NR	NR	NR

ACF: Aberrant crypt foci, AC: Aberrant crypt, ALP: Alkaline Phosphatase, CA125: Cancer antigen 125, CA153: Cancer antigen 153, CA199: Cancer antigen 199, CA242: Cancer Antigen 242, CEA: Carcinoembryonic antigen, CAMP: Campesterol, CAMS: Campestanol CAT: Catalase, Cav1: Caveolin 1, CMC: Carboxymethyl cellulose, CGLF: Colonic Glands in area of lymphoid follicle, DAU: Daucosterol, DAUL: Daucosterol linoleate, DAULN: Daucosterol linolenate, DAUP: Daucosterol palmitate, DU: Densitometry Unit, DW: Diet Weight, EGFR: Epidermal growth factor receptor, ER: Estrogen Receptor, ERK: Extracellular-signal-regulated kinase, FUCO: Fucosterol, GUGG: Guggulsterone GGT: Gamma glutamyl transferase, HFHC: High Fat High Cholesterol IP: Intraperitoneal injection, LDH: Lactate dehydrogenase, LFLC: Low Fat Low Cholesterol, MDA: malondialdehyde, MAPK: Mitogen-activated protein kinase, mg/kg.bw: milligrams per kilogram of body weight, n: number, NR: Not Reported, OG: Oral Gavage, PARP: Poly (ADP-ribose) polymerase, PCNA: Proliferating Cell Nuclear Antigen, PENI: Penicosterol, PO: Per Os, PSS: Phytosterols and stanols, PyMT antigen: Polyoma Virus Middle T antigen, SITO: β-Sitosterol, STIG: Stigmasterol, SI; Subcutaneous injection, SOD: Superoxide dismutase, VEGF: Vascular Endothelial Growth Factor, Wei: Weight. Dose mg/kg is per body weight per day unless otherwise stated. All protein presented as DU unless otherwise stated.Volume presented in cubic millimeter (mm3). Weight presented in grams (g). Area presented in square millimeter (mm2). Size presented in millimeter cubed (mm^3).

activation of oncogene expression and activity. The route of administration for high doses appeared to be an important determinant. The GI tract is exposed to highest doses of orally administered compounds, which may explain why dose equivalent to 70 g/person/day of plant stanols, or plant sterols, was associated with intestinal tumor formation. We are unaware of studies that have directly compared different routes of PSS administration to explore this hypothesis further. Globally, these data indicate that PSS dose, frequency and route of administration are likely to be important variables to consider in human studies, especially if pharmacological approaches with maximum tolerable doses are considered.

Resisting cell death

Programmed cell death is important for managing malignant and pre-malignant cells. Cancer cells become resistant to death signals by increasing the expression of anti-apoptotic proteins, and reducing expression of pro-apoptotic proteins. Bcl2 and Bclxl for example maintain mitochondrial membrane stability (thus preventing the release of cytochrome c into the cytoplasm, a very early event in apoptosis) and Bad and Bax oppose this mechanism by destabilizing mitochondrial membrane integrity. Caspases are then activated and enact orchestrated cellular destruction. In vivo, cell death can be assessed longitudinally by tumor growth assays, on flow sorted tumor cells labeled for various stages of apoptosis, or by measuring expression of proteins regulating apoptosis.

Across all studies we identified, tumors of PSS treated animals had significantly greater expression of pro-apoptotic proteins and reduced expression of anti-apoptotic signals (Figure 5). There was a significant decrease in expression of Bcl2 (SMD = −3.14; 95% CI: −5.40, −0.89; $p = 0.006$; Figure 5A) and BclxL (MD = −0.43 DU; 95% CI: −0.51, −0.35; $p < 0.0001$; Figure 5B) in the treated animals relative to controls. Both of these proteins function to maintain mitochondrial membrane integrity and resist apoptosis. For the pro-apoptotic proteins, Bax was strongly induced (SMD = 7.86; 95% CI: 2.69, 13.03; $p = 0.003$; Figure 5C), whilst Bad was also induced (MD = 0.14 DU; 95% CI: 0.07, 0.21; $p < 0.0001$ Figure 5D).

Downstream of mitochondrial membrane integrity regulation, caspase expression also regulates apoptosis. In PSS treated models Casp3 (SMD = 6.09; 95% CI: 2.04, 10.14; $p = 0.003$; Figure 5E) and Casp9 (SMD = 5.30; 95% CI: 1.74, 8.86; $p = 0.004$; Figure 5F) were both significantly higher than in controls. PSS derivatives appeared important in the magnitude of pro-apoptotic effect observed. Dolai et al., was the only study included using a PSS derivative, DAUC, and evaluated its effect on apoptosis proteins at 50 mg and 100 mg/kg per day IP. A clear dose dependant effect was seen with greater increase in cleaved Casp3 and Casp9, and Bax expression and decrease in anti-apoptotic Bcl2 in the highest treatment group (Table 1). Ma et al., established that either DAUC or DAUL at 60 mg/kg OG resulted in a greater Casp3 and Casp9 activation than SITO compared to the control untreated model, which was accompanied by significant decreases in PI3K/Akt signaling that were not present in the SITO group (Ma et al. 2019).

Other hallmarks

Proliferation and cell death were the most heavily studied hallmarks identified during the systematic search. Other hallmarks were less extensively studied, yet important discoveries have been made. Four studies measured markers of metastasis or direct metastatic colonization, and three evaluated markers of angiogenesis. PSS treated animals had significantly reduced metastatic colonization (SMD = −1.34; 95% CI: −1.91, −0.77; $p < 0.0001$; Figure 6A) from models of PCa (Awad et al. 2001), BCa (Han et al. 2018), and melanoma (Imanaka et al. 2008; Sundstrom et al. 2019). Matrix metalloproteinases (MMPs) enzymatic activity facilitate tumor invasion and metastatic process degrading the extracellular matrix (ECM) components, modulating cell adhesion and interfering with the biological activity of ECM components and other proteins. At the molecular level matrix metalloproteinase-2 (MMP2) and matrix metalloproteinase-9 (MMP9) were found significantly reduced in BCa xenograft models ($p < 0.00001$ for both; Figure 6B and C). Expression of Snail, a transcription factor that drives epithelial-mesenchymal transformation (EMT), was significantly reduced by SITO in PaCa BXPC3 xenografts, as were markers of EMT such as vimentin (Cao et al. 2018) (Table 1). ERK activation is associated with tumor cell angiogenesis and the metastatic EMT and Sharmila and Sindhu (2017b) found SITO reduced pERK. Sundstrom et al. (2019) also observed pERK reduction in brain metastases by SITO which was accompanied by fewer brain metastases in the PSS treated group (Sundstrom et al. 2019). Cao and colleagues evaluated GSK3β signaling in the context of metastasis formation and EMT in a PaCa xenograft model (Cao et al. 2018). SITO given daily by IP at 80 mg/kg significantly reduced E-cadherin and increased vimentin. The angiogenesis factor VEGF was reduced in the tumors of PSS treated mice, compared to controls, as observed in two separate BCa models (4T1 and MCF7), treated PO with 50 mg/kg and 100 mg/kg of DAUL (Han et al. 2018), and in a RCa model, treated with 20 mg/kg PO of SITO (Sharmila and Sindhu 2017a) ($p < 0.0001$; Figure 6D). Furthermore, STIG was shown to reduce CCA CD31+ vessels, suggesting a disruption in tumor blood vessel formation (Kangsamaksin et al. 2017) but not by a SITO:STIG:CAMP mixture in MMTV-PyMT Tg mice (Llaverias et al. 2013) (Table 1). Furthermore, only two studies were focused on tumor-promoting inflammation hallmark. Lipid peroxidation (LPO) is a mechanism that induces onset and progression of carcinogenesis through the production of reactive compounds like malondialdehyde (MDA). Ali et al. (2015) and Nguedia et al. (2020) showed that DMBA induced LPO, measured through MDA levels, is significantly reduced by STIG or DAUC relative to controls in mutagenic models of skin papilloma and breast cancer, respectively. However, while STIG increased the levels of superoxide dismutase (SOD), catalase (CAT) and the reduced form of glutathione (GSH), which are essential for reactive oxygen species (ROS) catalysis, DAUC increased only CAT activity (Nguedia et al. 2020), suggesting a weaker ability to induce endogenous antioxidant mechanisms compared to STIG.

Broad impact oncogenes

We found a number of oncogenes and tumor suppressor genes were evaluated as secondary endpoints in numerous studies. In vitro, PSS have been found to supress activity of AKT and NFκB pathways, and to act as PARP inhibitors, and these roles are evaluated here.

Excessive pAKT leads to enhanced tumor growth, resistance to death signals, metastasis, and angiogenesis (Revathidevi and Munirajan 2019). Our meta-analysis of 3 pAKT studies (n = 42 animals) indicated that pAKT levels were 45% lower in PSS treated groups (95% CI: −67%, −23%; $p < 0.0001$; Figure 7A). In our qualitive assessment, we noted that PI3K (an oncogene on the same pathway as AKT) was also downregulated (Han et al. 2018) and hypophosphorylated in PSS treated animals (Ma et al. 2019) (Table 1). Phosphorylation of NFκB's regulatory and transcription factor subunits was reduced by PSS in BCa and PaCa models. In BCa xenograft DAUL (100 mg/kg day; 7.5 g equ. human dose) reduced phosphorylation of IKKα/β, IkBa, and p65 (Han et al. 2018). In mammary gland extracts of the genetic BCa PyMT Tg model PSS treatment significantly impaired NFκB activity (Llaverias et al. 2013) under high fat diet conditions (Table 1). In the PaCa model, signaling by Nrf2-ARE was not altered by SITO, but NFκB activity was reduced. However, as reported earlier for proliferation, the CAMP rich high dose PSS mixture indicated that phytosterols given at high doses (20 mg per mouse per day) did not lead to suppression of oncogene expression or function (EGFR, b-catenin, cycline D1 or pERK) (Marttinen et al. 2014). Furthermore, the sister paper published the year before indicated that high phyto*stanol* (8 g/kg dw; 20 mg/day/mouse; 92% CAMS, 8% STAN) led to significant increases in pro-proliferative proteins including EGFR and Cyclin-D1 (Marttinen et al. 2013).

PARP is over expressed in many cancers and is a therapeutic target in the treatment of several cancer types with the use of PARP inhibitors. Our meta-analysis of 2 studies found nuclear PARP to be significantly reduced by PSS (SMD = −17.14; 95% CI: −24.03, −10.26; $p < 0.0001$ Figure 7B) (Couder-García et al. 2019; Ma et al. 2019) and cytoplasmic/cleaved PARP significantly increased (SMD = 6.22; 95% CI: 1.60, 10.83; $p = 0.008$ Figure 7C) (Han et al. 2018; Couder-García et al. 2019; Ma et al. 2019). HCT116 cells are Ataxia-Telangiectasia Mutated (ATM)-deficient indicating a sensitivity to DNA repair inhibiting drugs. Couder-Garcia and colleagues provided the only study that considered both dose and frequency of administration of PENI in mice xenograft model using HCT116 (Table 1). Interestingly PARP cleavage was strongly induced, and to a similar extent in both the frequent administration group (15 mg/kg 3 per week: 10.9-fold) and the high dose group (30 mg/kg once per week: 10.6-fold) (Han et al. 2018; Couder-García et al. 2019; Ma et al. 2019). As this study varied the frequency and dose of PENI administration it provided valuable information on how administration regimen should be considered in translational first-in-human studies.

The data described here suggests that PSS, particularly the glucoside derivatives of SITO, may be natural PARP inhibitors useful in the treatment of cancers characterized by mutations in DNA repair genes such as BRCA1/2. SITO, DAUC, and DAUL all influenced PARP activity by promoting significant decreases in nuclear (active) PARP, and increases in its cleaved (inactive) form.

Mechanistic insights

Several mechanistic insights into how PSS may alter proliferation of tumor cells were provided during the systematic review and details are reported in Table 1. Proliferation of estrogen receptor positive breast cancer MCF7 xenografts was inhibited by SITO provided in chow at 9.8 g/kg dw. Interestingly, SITO treatment led to 35% lower circulating levels of exogenously introduced estradiol, suggesting the antiproliferative actions of PSS could have been indirect via promoting estradiol clearance (Ju et al. 2004). Mitochondrial function was also found significantly impaired by SITO in a model of melanoma brain metastasis. In this study the authors discovered that mitochondrial membrane integrity was impaired by SITO and this led to oxidative stress mediated apoptosis (Sundstrom et al. 2019). The high PSS dose studies performed in the Apc^{min} mouse found increases in activity (phosphorylation) and expression of pro-proliferative oncogenes including EGFR, and ERK1/2. Activation of the same proteins, and others (c-jun, c-fos, JNK, and p38) in a KCa model was significantly reduced by prolonged exposure (44-weeks) to SITO (20 mg/kg PO 3 times/week) (Sharmila and Sindhu 2017b). These dose dependent differences in oncogene activation indicate a potential non-linear relationship, and activity and expression of such tumor markers should be assessed in clinical trials.

Evaluation of methodology

Heterogeneity

As expected, high levels of heterogeneity ($I^2 > 75\%$) were observed in the majority of our meta-analyses—all of which contained < 10 studies for each outcome. However, we also demonstrate consistent directionality of effects between studies within each meta-analysis. This suggests that despite *inter*-study differences in experimental design that underlie the high levels of heterogeneity, the administration of PSS consistently confers protective effects against the hallmarks of cancer. Although the present study was not powered to investigate sub-groups across most analyses, future studies may be adequately powered to identify key experimental features that drive heterogeneity.

Risk of bias and adherence to guidelines for reporting on natural products, animal research, and immunoblotting

According to BJP and PROSPERO guidelines for declaration of transparency and scientific rigor (BJP 2018a), animal research (BJP 2018b), use of natural products (BJP 2020), and use of immunoblotting and immunohistochemistry (BJP 2018c) we developed a 57 point survey (Figure 8) that was completed in duplicate by two independent researchers. Four papers did not report ethical approval for their research and corresponding authors did not respond via contact details provided in the manuscripts. Using our selection criteria, we had low risk of bias in terms of reporting study design (Figure 8A). Low ROB was also found for PSS origin, purity and measurement methods as these criteria were used to exclude manuscripts that did not report these characteristics, and/or evaluated effects of plant/food extracts rather than pure PSS. Few records evaluated PSS toxicity, pharmacokinetics, dosage rationale, or compared to clinically effective drug (Figure 8B). However, given the long-term use of PSS in the cardiovascular disease setting, these characteristics have been reported extensively elsewhere. Moreover, antibody validation was not reported in any study, immunoblots were always cropped (Figure 8C). We do not see this as a particular limitation here as antibodies against common oncogenes such as pAKT and VEGF have been extensively published previously.

Conclusions

SITO is the most common phytosterol found in foods and we found SITO was strongly associated with the inhibition of several cancer hallmarks including: resisting cell death, sustaining proliferative signaling, inducing angiogenesis, and activating invasion and metastasis (Graphical Abstract). SITO is abundant in healthy diets, especially in many vegetable oils (500 mg sterol per 100 g oil), cereals (50 mg/100g), and nuts (200 mg/100g) (Yang et al. 2019). However, given the wide range of PSS available in nature, over 200 different PSS have now been identified and classified (Moreau et al. 2018) it may be important to determine whether any of these PSS that are as yet untested as anti-tumor agents, could be better suited. The evidence provided here that SITO at physiologically achievable concentrations significantly impairs tumor development supports the argument that clinical trials should be evaluating its efficacy as an adjunct to existing treatment. If translatable to humans, the evidence presented here suggests that relatively modest (>200 mg) daily PSS intake could impair oncogenic signaling and suppression of multiple cancer hallmarks leading to reduced cancer risk. Indeed a distinction should be made between cancer prevention using dietary advice, and cancer treatment using nutraceutical approaches.

We also have found convincing evidence that PSS may synergise with several existing therapies such as PARP inhibitors (Couder-García et al. 2019), gemcitabine (Cao et al. 2018), and vemurafenib (Sundstrom et al. 2019). However, the cellular receptors for PSS have not been clearly identified in the context of cancer cell biology. Previously, PSS was shown to dampen the effect of oxysterols in breast cancer (Hutchinson et al. 2019), and oxysterols are now considered strong mediators of the pathophysiology of several cancers (Baek et al. 2017; Segala et al. 2017; He et al. 2019). Further mechanistic evidence could be provided by applying emerging technologies such as phage display high throughput screens (Dilly et al. 2017) to panels of PSS to identify cellular protein receptors to which PSS directly bind. An alternative mechanism of action is integration into cellular membranes. Disruption of the plasma membrane would impair signaling by oncogenic signaling pathways including AKT (Fakih et al. 2018), and disruption of mitochondrial membrane integrity promotes oxidative stress and tumor cell specific apoptosis (Sundstrom et al. 2019). Given the well understood toxicity profile of PSS, combined with their now >20-year use in clinic to reduce cardio-vascular disease risk, and the plethora of preclinical in vivo evidence we have summarized here, it is timely to consider PSS as adjuncts to cancer therapies.

Competing interests

No potential conflict of interest was reported by the authors.

Abbreviations

ACF	Aberrant Crypt Foci;
AWH	Average weight human (70kg);
BCa	Breast Cancer;
BRAS	Dihydrobrassicasterol;
CA125	Cancer antigen 125;
CA153	Cancer antigen 153;
CA199	Cancer antigen 199;
CA242	Cancer Antigen 242;
Cav1	Caveolin 1;
CEA	Carcinoembryonic antigen;
CCA	Cholangiocarcinoma;
CAT	Catalase;
CGLF	Colonic Glands in area of lymphoid follicle;
CAMP	Campesterol;
CAMS	Campestanol;
CI	confidence interval;
CRC	Colorectal Cancer;
DAUC	Daucosterol a.k.a β-Sitosterol glucoside;
DAUL	Daucosterol Linoleate or β-Sitosterol-Glucoside Linoleate;
DAUN	Daucosterol linolenate;
DAUP	Daucosterol Palmitate;
DU	Densitometry Unit;
dw	dry weight;
EFSA	European Food Standards Agency;
EGFR	Epidermal growth factor receptor;
EMT	Epithelial Mesenchymal Transition;
ER	Estrogen Receptor;
ERK	Extracellular-signal-regulated kinase;
E2	Estradiol;
ECa	Ehrlich-Lettre ascites carcinoma;
EMT	epithelial-mesenchymal transformation;
FUCO	Fucosterol;
GGT	Gamma glutamyl transferase;
GSH	glutathione;
HFHC	High Fat High Cholesterol;
HEP	Hepatoma;
IP	intraperitoneal;
IV	intravenous;
LCa	Lung Cancer;
LDH	Lactate dehydrogenase;
LDL-C	low density lipoprotein cholesterol;
LFLC	Low Fat Low Cholesterol;
MAPK	Mitogen-activated protein kinase;
MNU	N-methyl-N-nitrosourea;
MDA	malondialdehyde;
MDSC	Myeloid-Derived Suppressor Cells;
n	number;
MMP2	matrix metalloproteinase-2;
MMP9	matrix metalloproteinase-9;
NR	Not Reported;
NF-κB	Nuclear Factor Kappa Beta;
NOAEL	No Observed Adverse Effect Level;
OCa	Ovarian Cancer;
OG	Oral gavage;
PaCa	Pancreatic Cancer;
PCa	Prostate Cancer;
PARP	Poly (ADP-ribose) polymerase;
PCNA	Proliferating Cell Nuclear Antigen;
PENI	Peniocerol;
PO	per oral;
PSS	Phytosterols and stanols;
PyMT antigen	
Polyoma Virus Middle T antigen;	
PSTE	Plant Sterol Esters;
P4	Progesterone;
RCa	Renal Cancer = ROS = Reactive Oxygen Species;
SCa	Skin Cancer or Melanoma;
SCFA	Short Chain Fatty Acids;
SITO	β-Sitosterol;
STAN	Sitostanol;
STIG	Stigmasterol;
SI	Subcutaneous injection;
SOD	Superoxide dismutase;
TSP-1	Thrombospondin-1;
VEGF	Vascular Endothelial Growth Factor;
ZGUG	Z-Guggulsterone;
Wei	Weight.

Funding

GC is supported by a research grant from Breast Cancer Action (3T57/9R17-02). CS and AW are supported by doctoral scholarships from the University of Leeds.

ORCID

Giorgia Cioccoloni http://orcid.org/0000-0003-0102-9182
Chrysa Soteriou http://orcid.org/0000-0002-2808-1215
Alex Websdale http://orcid.org/0000-0002-6147-933X
Lewis Wallis http://orcid.org/0000-0001-5800-3245
Michael A. Zulyniak http://orcid.org/0000-0003-4944-5521
James L. Thorne http://orcid.org/0000-0002-3037-8528

References

Ali, H., S. Dixit, D. Ali, S. M. Alqahtani, S. Alkahtani, and S. Alarifi. 2015. Isolation and evaluation of anticancer efficacy of stigmasterol in a mouse model of DMBA-induced skin carcinoma. *Drug Design, Development and Therapy* 9:2793–800.

Alrawi, S. J., M. Schiff, R. E. Carroll, M. Dayton, J. F. Gibbs, M. Kulavlat, D. Tan, K. Berman, D. L. Stoler, and G. R. Anderson. 2006. Aberrant crypt foci. *Anticancer Research* 26 (1A):107–19.

An, M. J., J. H. Cheon, S. W. Kim, E. S. Kim, T. I. Kim, and W. H. Kim. 2009. Guggulsterone induces apoptosis in colon cancer cells and inhibits tumor growth in murine colorectal cancer xenografts. *Cancer Letters* 279 (1):93–100. doi:10.1016/j.canlet.2009.01.026.

Awad, A. B., C. S. Fink, H. Williams, and U. Kim. 2001. In vitro and in vivo (SCID mice) effects of phytosterols on the growth and dissemination of human prostate cancer PC-3 cells. European *Journal of Cancer Prevention* 10 (6):507–13.

Bae, H., J.-Y. Lee, G. Song, and W. Lim. 2020. Fucosterol Suppresses the Progression of Human Ovarian Cancer by Inducing

Mitochondrial Dysfunction and Endoplasmic Reticulum Stress. *Marine Drugs* 18 (5):261 doi:10.3390/md18050261.

Baek, A. E., Y. A. Yu, S. He, S. E. Wardell, C. Y. Chang, S. Kwon, R. V. Pillai, H. B. McDowell, J. W. Thompson, L. G. Dubois, et al. 2017. The cholesterol metabolite 27 hydroxycholesterol facilitates breast cancer metastasis through its actions on immune cells. *Nature Communications* 8 (1):864. doi: 10.1038/s41467-017-00910-z.

Baskar A. A., S. Ignacimuthu, G. M. Paulraj, and K. S. Al Numair. 2010. Chemopreventive potential of β-Sitosterol in experimental colon cancer model - an *In vitro* and *In vivo* study. *BMC Complementary and Alternative Medicine*. doi:10.1186/1472-6882-10-24. PMID: 20525330.

BJP. 2018a. Declaration of transparency and scientific rigour: Checklist for design & analysis. *British Journal of Pharmacology* 175 (13):2709.

BJP. 2018b. Declaration of transparency and scientific rigour: Checklist for animal experimentation. *British Journal of Pharmacology* 175 (13):2711.

BJP. 2018c. Declaration of transparency and scientific rigour: Checklist for immunoblotting and immunohistochemistry. *British Journal of Pharmacology* 175 (13):2710.

BJP. 2020. Declaration of transparency and scientific rigour: Checklist for reproducibility of natural product research. *British Journal of Pharmacology*. 177 (10):2179.

Borenstein, M., L. V. Hedges, J. P. T. Higgins, and H. R. Rothstein. 2009. Effect sizes based on means. In *Introduction to meta-analysis*, 21–32.

Cao, Z. Q., X. X. Wang, L. Lu, J. W. Xu, X. B. Li, G. R. Zhang, Z. J. Ma, A. C. Shi, Y. Wang, and Y. J. Song. 2018. β-sitosterol and gemcitabine exhibit synergistic anti-pancreatic cancer activity by modulating apoptosis and inhibiting epithelial-mesenchymal transition by deactivating Akt/GSK-3β signaling. *Frontiers in Pharmacology* 9: 1525. doi: 10.3389/fphar.2018.01525.

Couder-García, B. D. C., N. J. Jacobo-Herrera, A. Zentella-Dehesa, L. Rocha-Zavaleta, Z. Tavarez-Santamaría, and M. Martínez-Vázquez. 2019. The phytosterol peniocerol inhibits cell proliferation and tumor growth in a colon cancer xenograft model. Frontiers *in Oncology* 9:1341.

De Stefani, E., P. Boffetta, A. L. Ronco, P. Brennan, H. Deneo-Pellegrini, J. C. Carzoglio, and M. Mendilaharsu. 2000. Plant sterols and risk of stomach cancer: A case-control study in Uruguay. *Nutrition and Cancer* 37 (2):140–4. doi: 10.1207/S15327914NC372_4.

Deeks, J. J., J. P. T. Higgins, and D. G. Altman. 2019. Cochrane handbook for systematic reviews of interventions. John Wiley & Sons.

Deschner, E. E., B. I. Cohen, and R. F. Raicht. 1982. The kinetics of the protective effect of?-sitosterol against MNU-induced colonic neoplasia. *Journal of Cancer Research and Clinical Oncology* 103 (1): 49–54. doi:10.1007/BF00410305.

Dilly, S. J., A. J. Clark, A. Marsh, D. A. Mitchell, R. Cain, C. W. G. Fishwick, and P. C. Taylor. 2017. A chemical genomics approach to drug reprofiling in oncology: Antipsychotic drug risperidone as a potential adenocarcinoma treatment. *Cancer Letters* 393:16–21. doi: 10.1016/j.canlet.2017.01.042.

Dolai, N., A. Kumar, A. Islam, and P. K. Haldar. 2016. Apoptogenic effects of β-sitosterol glucoside from Castanopsis indica leaves. *Natural Product Research* 30 (4):482–5. doi:10.1080/14786419.2015.1023201.

EFSA Panel on Dietetic Products, Nutrition and Allergies. 2013. Scientific Opinion on the substantiation of a health claim related to the consumption of 2 g/day of plant stanols (as plant stanol esters) as part of a diet low in saturated fat and a two-fold greater reduction in blood LDL-cholesterol concentrations compared to the consumption of a diet low in saturated fat alone pursuant to Article 14 of Regulation (EC) No 1924/2006. *EFSA Journal* 11 (4).

Fakih, O., D. Sanver, D. Kane, and J. L. Thorne. 2018. Exploring the biophysical properties of phytosterols in the plasma membrane for novel cancer prevention strategies. *Biochimie* 153:150–61. doi: 10.1016/j.biochi.2018.04.028.

Han, B., P. Jiang, W. Liu, H. Xu, Y. Li, Z. Li, H. Ma, Y. Yu, X. Li, and X. Ye. 2018. Role of daucosterol linoleate on breast cancer: Studies on apoptosis and metastasis. *Journal of Agricultural and Food Chemistry* 66 (24):6031–41. doi: 10.1021/acs.jafc.8b01387.

Han, S., J. Jiao, J. Xu, D. Zimmermann, L. Actis-Goretta, L. Guan, Y. Zhao, and L. Qin. 2016. Effects of plant stanol or sterol-enriched diets on lipid profiles in patients treated with statins: Systematic review and meta-analysis. *Scientific Reports* 6:31337. doi: 10.1038/srep31337.

Hanahan, D., and R. A. Weinberg. 2000. The hallmarks of cancer. *Cell* 100 (1):57–70. doi: 10.1016/S0092-8674(00)81683-9.

Hanahan, D., and R. A. Weinberg. 2011. Hallmarks of cancer: The next generation. *Cell* 144 (5):646–74. doi: 10.1016/j.cell.2011.02.013.

He, S., L. Ma, A. E. Baek, A. Vardanyan, V. Vembar, J. J. Chen, A. T. Nelson, J. E. Burdette, and E. R. Nelson. 2019. Host CYP27A1 expression is essential for ovarian cancer progression. *Endocrine-Related Cancer* 26 (7):659–75. doi: 10.1530/ERC-18-0572.

Huang, J., M. Xu, Y. J. Fang, M. S. Lu, Z. Z. Pan, W. Q. Huang, Y. M. Chen, and C. X. Zhang. 2017. Association between phytosterol intake and colorectal cancer risk: A case-control study. *British Journal of Nutrition* 117 (6):839–50. doi: 10.1017/S0007114517000617.

Hutchinson, S. A., P. Lianto, J. B. Moore, T. A. Hughes, and J. L. Thorne. 2019. Phytosterols inhibit side-chain oxysterol mediated activation of LXR in breast cancer cells. *International Journal of Molecular Sciences* 20 (13):3241 doi:10.3390/ijms20133241.

Imanaka, H., H. Koide, K. Shimizu, T. Asai, N. Kinouchi Shimizu, A. Ishikado, T. Makino, and N. Oku. 2008. Chemoprevention of tumor metastasis by liposomal beta-sitosterol intake. *Biological & Pharmaceutical Bulletin* 31 (3):400–4. doi: 10.1248/bpb.31.400.

Iyer, D., and U. K. Patil. 2012. Efficacy of stigmast-5-en-3β-ol isolated from *Salvadora persica* L. as antihyperlipidemic and anti-tumor agent: Evidence from animal studies. *Asian Pacific Journal of Tropical Disease* 2 (Suppl 2):S849–S855. doi: 10.1016/S2222-1808(12)60278-3.

Jackson, D., and R. Turner. 2017. Power analysis for random-effects meta-analysis. *Research Synthesis Methods* 8 (3):290–302. doi: 10.1002/jrsm.1240.

Janezic, S. A., and A. V. Rao. 1992. Dose-dependent effects of dietary phytosterol on epithelial cell proliferation of the murine colon. *Food and Chemical Toxicology* 30 (7):611–6. doi: 10.1016/0278-6915(92)90195-Q.

Jiang, P., B. Han, L. Jiang, Y. Li, Y. Yu, H. Xu, Z. Li, D. Zhou, X. Jia, X. Li, et al. 2019. Simultaneous separation and quantitation of three phytosterols from the sweet potato, and determination of their anti-breast cancer activity. *Journal of Pharmaceutical and Biomedical Analysis* 174:718–27. doi:10.1016/j.jpba.2019.06.048.

Jiang, L., X. Zhao, J. Xu, C. Li, Y. Yu, W. Wang, and L. Zhu. 2019. The protective effect of dietary phytosterols on cancer risk: A systematic meta-analysis. Journal *of Oncology* 2019:1–11. doi: 10.1155/2019/7479518.

Ju, Y. H., L. M. Clausen, K. F. Allred, A. L. Almada, and W. G. Helferich. 2004. β-sitosterol, β-sitosterol glucoside, and a mixture of β-sitosterol and β-sitosterol glucoside modulate the growth of estrogen-responsive breast cancer cells in vitro and in ovariectomized athymic mice. *The Journal of Nutrition* 134 (5):1145–51. doi: 10.1093/jn/134.5.1145.

Kangsamaksin, T., S. Chaithongyot, C. Wootthichairangsan, R. Hanchaina, C. Tangshewinsirikul, and J. Svasti. 2017. Lupeol and stigmasterol suppress tumor angiogenesis and inhibit cholangiocarcinoma growth in mice via downregulation of tumor necrosis factor-α. *PLoS One* 12 (12):e0189628. doi: 10.1371/journal.pone.0189628.

Kazłowska, K., H. T. V. Lin, S. H. Chang, and G. J. Tsai. 2013. In vitro and in vivo anticancer effects of sterol fraction from red algae porphyra dentata. *Evidence-Based Complementary and Alternative Medicine* 2013:1–10. doi: 10.1155/2013/493869.

Llaverias, G., J. C. Escolà-Gil, E. Lerma, J. Julve, C. Pons, A. Cabré, M. Cofán, E. Ros, J. L. Sánchez-Quesada, and F. Blanco-Vaca. 2013. Phytosterols inhibit the tumor growth and lipoprotein oxidizability induced by a high-fat diet in mice with inherited breast cancer. *The Journal of Nutritional Biochemistry* 24 (1):39–48. doi: 10.1016/j.jnutbio.2012.01.007.

Ma, H., Y. Yu, M. Wang, Z. Li, H. Xu, C. Tian, J. Zhang, X. Ye, and X. Li. 2019. Correlation between microbes and colorectal cancer: Tumor apoptosis is induced by sitosterols through promoting gut microbiota to produce short-chain fatty acids. *Apoptosis* 24 (1-2): 168–83. doi: 10.1007/s10495-018-1500-9.

Mao, Z., X. Shen, P. Dong, G. Liu, S. Pan, X. Sun, H. Hu, L. Pan, and J. Huang. 2019. Fucosterol exerts antiproliferative effects on human lung cancer cells by inducing apoptosis, cell cycle arrest and targeting of Raf/MEK/ERK signalling pathway. *Phytomedicine*. doi: 10.1016/j.phymed.2018.12.032.

Marttinen, M., E. Päivärinta, M. Storvik, L. Huikko, H. Luoma-Halkola, V. Piironen, A. M. Pajari, and M. Mutanen. 2013. Plant stanols induce intestinal tumor formation by up-regulating Wnt and EGFR signaling in Apc Min mice. *Journal of Nutritional Biochemistry* 24 (1):343–52. doi: 10.1016/j.jnutbio.2012.07.002.

Marttinen, M., A. M. Pajari, E. Päivärinta, M. Storvik, P. Marttinen, T. Nurmi, M. Niku, V. Piironen, and M. Mutanen. 2014. Plant sterol feeding induces tumor formation and alters sterol metabolism in the intestine of Apc(Min) mice. *Nutrition and Cancer* 66 (2):259–69. doi: 10.1080/01635581.2014.865244.

McCann, S. E., J. L. Freudenheim, J. R. Marshall, and S. Graham. 2003. Risk of human ovarian cancer is related to dietary intake of selected nutrients, phytochemicals and food groups. *The Journal of Nutrition* 133 (6):1937–42. doi: 10.1093/jn/133.6.1937.

Mendilaharsu, M., E. De Stefani, H. Deneo-Pellegrini, J. Carzoglio, and A. Ronco. 1998. Phytosterols and risk of lung cancer: A case-control study in Uruguay. *Lung Cancer* 21 (1):37–45. doi: 10.1016/S0169-5002(98)00044-0.

Moreau, R. A., L. Nystrom, B. D. Whitaker, J. K. Winkler-Moser, D. J. Baer, S. K. Gebauer, and K. B. Hicks. 2018. Phytosterols and their derivatives: Structural diversity, distribution, metabolism, analysis, and health-promoting uses. *Progress in Lipid Research* 70:35–61. doi: 10.1016/j.plipres.2018.04.001.

Nguedia, M. Y., A. B. Tueche, A. J. G. Yaya, V. Yadji, D. T. Ndinteh, D. Njamen, and S. Zingue. 2020. Daucosterol from *Crateva adansonii* DC (Capparaceae) reduces 7,12-dimethylbenz(a)anthracene-induced mammary tumors in Wistar rats. *Environmental Toxicology* 35 (10):1125–36. doi: 10.1002/tox.22948.

Peter, E. L., A. G. Mtewa, P. B. Nagendrappa, A. Kaligirwa, and C. D. Sesaazi. 2020. Systematic review and meta-analysis protocol for efficacy and safety of *Momordica charantia* L. on animal models of type 2 diabetes mellitus. *Systematic Reviews* 9 (1):7. doi: 10.1186/s13643-019-1265-4.

Phillips, K. M., D. M. Ruggio, and M. Ashraf-Khorassani. 2005. Phytosterol composition of nuts and seeds commonly consumed in the United States. *Journal of Agricultural and Food Chemistry* 53 (24): 9436–9445.

Quilliot, D., F. Boman, C. Creton, X. Pelletier, J. Floquet, and G. Debry. 2001. Phytosterols have an unfavourable effect on bacterial activity and no evident protective effect on colon carcinogenesis. *European Journal of Cancer Prevention* 10 (3):237–43.

Revathidevi, S., and A. K. Munirajan. 2019. Akt in cancer: Mediator and more. *Seminars in Cancer Biology* 59:80–91. doi: 10.1016/j.semcancer.2019.06.002.

Rohatgi, A. 2019. WebPlotDigitizer (v4.2). https://automeris.io/WebPlotDigitizer

Segala, G., M. David, P. de Medina, M. C. Poirot, N. Serhan, F. Vergez, A. Mougel, E. Saland, K. Carayon, J. Leignadier, et al. 2017. Dendrogenin A drives LXR to trigger lethal autophagy in cancers. *Nature Communications* 8 (1):1903. doi: 10.1038/s41467-017-01948-9.

Sharmila, R., and G. Sindhu. 2017a. Evaluate the antigenotoxicity and anticancer role of β-sitosterol by determining oxidative DNA damage and the expression of phosphorylated mitogen-activated protein kinases', C-fos, C-jun, and endothelial growth factor receptor. Pharmacognosy *Magazine* 13 (49):95–101.

Sharmila, R., and G. Sindhu. 2017b. Modulation of angiogenesis, proliferative response and apoptosis by β-sitosterol in rat model of renal carcinogenesis. *Indian Journal of Clinical Biochemistry* 32 (2): 142–52. doi: 10.1007/s12291-016-0583-8.

Shin, E. J., H.-K. Choi, M. J. Sung, J. H. Park, M.-Y. Chung, S. Chung, and J.-T. Hwang. 2018. Anti-tumour effects of beta-sitosterol are mediated by AMPK/PTEN/HSP90 axis in AGS human gastric adenocarcinoma cells and xenograft mouse models. *Biochemical Pharmacology* 152:60–70. doi:10.1016/j.bcp.2018.03.010.

Sofi M. S., M. K. Sateesh, M. Bashir, M. A. Ganie, and S. Nabi. 2018. Chemopreventive and anti-breast cancer activity of compounds isolated from leaves of Abrus precatorius L. *3 Biotech*. 8(8):371. doi: 10.1007/s13205-018-1395-8.

Sundstrom, T., L. Prestegarden, F. Azuaje, S. N. Aasen, G. V. Rosland, J. K. Varughese, M. Bahador, S. Bernatz, Y. Braun, P. N. Harter, et al. 2019. Inhibition of mitochondrial respiration prevents BRAF-mutant melanoma brain metastasis. *Acta Neuropathologica Communications* 7 (1):55. doi: 10.1186/s40478-019-0712-8.

The Nordic Cochrane Centre, T. C. C. 2014. Review Manager (RevMan) [Computer program].

Thorne, J. L., G. Cioccoloni, L. Wallis, A. Websdale, C. Soteriou, and M. Zulyniak. 2020. Phytosterols and phytostanols (PSS) and the hallmarks of cancer: A systematic review of evidence from pre-clinical models. PROSPERO: International prospective register of systematic reviews. PROSPERO.

Vesterinen, H. M., E. S. Sena, K. J. Egan, T. C. Hirst, L. Churolov, G. L. Currie, A. Antonic, D. W. Howells, and M. R. Macleod. 2014. Meta-analysis of data from animal studies: A practical guide. *Journal of Neuroscience Methods* 221:92–102. doi: 10.1016/j.jneumeth.2013.09.010.

Wang, X., M. Li, M. Hu, P. Wei, and W. Zhu. 2017. BAMBI overexpression together with β-sitosterol ameliorates NSCLC via inhibiting autophagy and inactivating TGF-β/Smad2/3 pathway. *Oncology Reports* 37 (5):3046–54. doi:10.3892/or.2017.5508.

WCRF/AICR. 2018. *Diet, nutrition, physical activity and cancer: A global perspective. Continuous update project expert report 2018*. London: World Cancer Research Fund/American Institute for Cancer Research.

Yaacob, N. S., H. M. Yankuzo, S. Devaraj, J. K. M. Wong, and C. S. Lai. 2015. Anti-tumor action, clinical biochemistry profile and phytochemical constituents of a pharmacologically active fraction of *S. crispus* in NMU-induced rat mammary tumour model. *PLoS One* 10 (5):e0126426. doi: 10.1371/journal.pone.0126426.

Yang, R., L. Xue, L. Zhang, X. Wang, X. Qi, J. Jiang, L. Yu, X. Wang, W. Zhang, Q. Zhang, et al. 2019. Phytosterol contents of edible oils and their contributions to estimated phytosterol intake in the Chinese diet. *Foods* 8 (8):334. doi: 10.3390/foods8080334.

Zhao, C., T. She, L. Wang, Y. Su, L. Qu, Y. Gao, S. Xu, S. Cai, and C. Shou. 2015. Daucosterol inhibits cancer cell proliferation by inducing autophagy through reactive oxygen species-dependent manner. *Life Sciences* 137:37–43. doi:10.1016/j.lfs.2015.07.019.